Received: 1 August 2022 | Revised: 23 December 2022 | Accepted: 28 December 2022

DOI: 10.1111/1755-0998.13750

MOLECULAR ECOLOGY RESOURCES WILEY

RESOURCE ARTICLE

A chromosome-level genome assembly enables the identification of the follicule stimulating hormone receptor as the master sex-determining gene in the flatfish *Solea senegalensis*

Roberto de la Herrán[1] | Miguel Hermida[2] | Juan Andres Rubiolo[2] | Jèssica Gómez-Garrido[3] | Fernando Cruz[3] | Francisca Robles[1] | Rafael Navajas-Pérez[1] | Andres Blanco[2] | Paula Rodriguez Villamayor[2] | Dorinda Torres[2] | Pablo Sánchez-Quinteiro[4] | Daniel Ramirez[5] | Maria Esther Rodríguez[5] | Alberto Arias-Pérez[5] | Ismael Cross[5] | Neil Duncan[6] | Teresa Martínez-Peña[7] | Ana Riaza[7] | Adrian Millán[8] | M. Cristina De Rosa[9] | Davide Pirolli[9] | Marta Gut[3] | Carmen Bouza[2] | Diego Robledo[10] | Laureana Rebordinos[5] | Tyler Alioto[3,11] | Carmelo Ruíz-Rejón[1] | Paulino Martínez[2]

[1]Departamento de Genética, Facultad de Ciencias, Universidad de Granada, Granada, Spain

[2]Departamento de Zoología, Genética y Antropología Física; Facultad de Veterinaria, Universidade de Santiago de Compostela, Lugo, Spain

[3]Centre Nacional d'Anàlisi Genòmica (CNAG-CRG), Centre de Regulació Genómica, Parc Científic de Barcelona, Barcelona, Spain

[4]Departamento de Anatomía, Producción Animal y Ciencias Clínicas Veterinarias Facultad de Veterinaria, Universidade de Santiago de Compostela, Lugo, Spain

[5]Departamento de Biomedicina, Biotecnología y Salud Pública CASEM – Facultad de Ciencias del Mar y Ambientales, Universidad de Cádiz, Cádiz, Spain

[6]IRTA Sant Carles de la Rapita, Tarragona, Spain

[7]Stolt Sea Farm SA, Departamento I+D, A Coruña, Spain

[8]Geneaqua SL, Lugo, Spain

[9]Institute of Chemical Sciences and Technologies "Giulio Natta" (SCITEC) – CNR c/o Catholic University of Rome, Rome, Italy

[10]The Roslin Institute and Royal (Dick) School of Veterinary Studies, University of Edinburgh, Midlothian, UK

[11]Universitat Pompeu Fabra (UPF), Barcelona, Spain

Correspondence
Paulino Martínez, Departamento de Zoología, Genética y Antropología Física, Facultad de Veterinaria, Universidade de Santiago de Compostela, Campus de Lugo, 27002 Lugo, Spain.
Email: paulino.martinez@usc.es

Funding information
European Union's Horizon 2020 research and innovation programme under grant agreement (AQUA-FAANG), Grant/Award Number: 81792; Junta de Andalucía-

Abstract

Sex determination (SD) shows huge variation among fish and a high evolutionary rate, as illustrated by the Pleuronectiformes (flatfishes). This order is characterized by its adaptation to demersal life, compact genomes and diversity of SD mechanisms. Here, we assembled the *Solea senegalensis* genome, a flatfish of great commercial value, into 82 contigs (614 Mb) combining long- and short-read sequencing, which were next scaffolded using a highly dense genetic map (28,838 markers, 21 linkage groups), representing 98.9% of the assembly. Further, we established the correspondence

Roberto de la Herrán, Miguel Hermida and Juan Andres Rubiolo contributed equally to this work.

FEDER Grant, Grant/Award Number: P20-00938; Spanish Ministry of Economy and Competitiveness, FEDER Grants, Grant/Award Number: RTI2018-096847-B-C21 and RTI2018-096847-B-C22; Ministry of Economy and Competitiveness; Junta de Andalucía; European Union; Horizon 2020

Handling Editor: Andrew DeWoody

between the assembly and the 21 chromosomes by using BAC-FISH. Whole genome resequencing of six males and six females enabled the identification of 41 single nucleotide polymorphism variants in the follicle stimulating hormone receptor (*fshr*) consistent with an XX/XY SD system. The observed sex association was validated in a broader independent sample, providing a novel molecular sexing tool. The *fshr* gene displayed differential expression between male and female gonads from 86 days post-fertilization, when the gonad is still an undifferentiated primordium, concomitant with the activation of *amh* and *cyp19a1a*, testis and ovary marker genes, respectively, in males and females. The Y-linked *fshr* allele, which included 24 nonsynonymous variants and showed a highly divergent 3D protein structure, was overexpressed in males compared to the X-linked allele at all stages of gonadal differentiation. We hypothesize a mechanism hampering the action of the follicle stimulating hormone driving the undifferentiated gonad toward testis.

KEYWORDS
follicule stimulating hormone receptor, genetic map, Senegalese sole, sex determination, whole genome sequencing

1 | INTRODUCTION

Sex determination (SD) refers to the mechanism controlling the fate of the gonadal primordium at the initial stages of development responsible for the sex of a mature individual. While highly conserved and evolutionary mature SD systems have been reported in mammals and birds, increasing data from ectothermic vertebrates provide a sharply different picture (Guiguen et al., 2019; Martínez et al., 2014). Fish display highly diverse chromosome SD systems (Cioffi et al., 2017) and several master SD genes have been reported in this group (Martínez et al., 2014). Among them are: classical transcription factors such as *dmy* (Matsuda et al., 2002; Wang et al., 2022), *sox3* (Takehana et al., 2014) or *sox2* (Martínez et al., 2021); transforming growth factor β-related genes such as *gsdf* (Herpin et al., 2021; Myosho et al., 2012) or *amh* (Hattori et al., 2012; Pan et al., 2019) and its receptor *amhr2* (Feron et al., 2020; Kamiya et al., 2012; Nacif et al., 2022; Nakamoto et al., 2021; Wen et al., 2022; Zheng et al., 2022); genes related to the steroidogenic pathway such as *bcar1* (Bao et al., 2019) or *hsd17b1* (Koyama et al., 2019); and, finally, some unexpected, such as the interferon-related *sdY* gene in salmonids (Yano et al., 2013). The recent identification of several master SD genes in this group has been associated with the highly contiguous and reliable chromosome-level genome assemblies achieved via improvements in long-read sequencing technologies, scaffolding and bioinformatic approaches (Ramos & Antunes, 2022).

Flatfish (Pleuronectiformes) represent a fish order with notable adaptations to demersal life (Chen et al., 2014; Figueras et al., 2016; Lü et al., 2021; Robledo et al., 2016; Shao et al., 2017). They experience a remarkable metamorphosis from the bilateral morphology of pelagic larvae to the flat morphology typical of this group (Lü et al., 2021; Shao et al., 2017). The adaptation to a demersal lifestyle promoted rapid diversification, reflected by a higher molecular evolutionary rate than their bilateral counterparts (Lü et al., 2021). This rapid radiation also led to a large variety of SD mechanisms, involving different master SD genes and non-orthologous SD regions in all species analysed to date (Luckenbach et al., 2009; Martínez et al., 2021). Flatfish genomes are compact (~500–700 Mb; Robledo et al., 2017; Lü et al., 2021), which has facilitated chromosome-level genome assemblies in species from several families of the order (Guerrero-Cózar et al., 2021; Lü et al., 2021; Martínez et al., 2021).

Solea *senegalensis* is a valuable commercial flatfish which lives on sandy or muddy bottoms, from brackish lagoons and shallow waters to deeper coastal regions (Cabral, 2000; Díaz-Ferguson et al., 2012). Further, it is a very promising aquaculture species (currently ~2000 tons; Ana Riaza, pers. comm.), which has promoted the development of a number of genomic resources and tools in the last decade (Robledo et al., 2017), including a recent whole genome assembly (Guerrero-Cózar et al., 2021). The species shows high larval survival rates as compared to other flatfish, such as turbot, and great capacity for adjusting to intensive production, the commercial size being reached at the age of 1 year (Morais et al., 2016). Females show higher growth rate than males and mature at 3 years of age, while males do so at 2 years (Viñas et al., 2013), so obtaining all-female populations is an appealing strategy to increase growth rate at farms. As with other Pleuronectiformes, the Senegalese sole undergoes a process of metamorphosis at 10–12 dph (days post-hatching) and for about 7 days to acquire the typical asymmetry adapted to the benthic lifestyle of flatfish (Martín et al., 2019). An important limitation for the expansion of *S. senegalensis* aquaculture regards the low performance of F_1 males (born and reared in captivity) compared to wild specimens reared in captivity, hampering the development of breeding programmes (Martín et al., 2019). Recently,

Guerrero-Cózar et al. (2021) identified the follicule stimulating hormone receptor as a candidate SD-determining gene using RADseq but highlighted the need for further validation including functional data. Understanding the mechanisms underlying reproduction, including the SD mechanism, and how external cues are connected to gonad development via neural communication, will be essential to boost *S. senegalensis* aquaculture. Here, we constructed a new highly contiguous genome assembly in *S. senegalensis* and integrated all mapping resources (physical, genetic and cytogenetic), thus providing a robust framework for evolutionary genomics in pleuronectiforms and teleosts. This assembly was used to identify the putative master SD gene of the species, the follicle stimulating hormone receptor (*fshr*), by resequencing a sample of males and females. The pattern of variation observed confirmed an XX/XY system and enabled the development of a molecular tool for sex determination in this species. Functional differences between male and female gonads were evaluated throughout gonad development, from the undifferentiated primordium to maturation. Our study, supported by gene expression data, three-dimensional protein structure predictions and whole genome resequence analysis of males and females, suggests that a functionally divergent, overexpressed Y-linked allele of the follicle stimulating hormone receptor (*fshry*) may determine the testis fate of the undifferentiated primordium in *S. senegalensis*.

2 | MATERIALS AND METHODS

2.1 | Samples

Biological and genomic metadata of *Solea senegalensis* samples analysed in this study are given in the supporting Table Metadata.

2.2 | DNA sequencing

2.2.1 | Long-read whole genome sequencing

High-molecular-weight DNA was purified from one female of *S. senegalensis* whole blood using the Nanobind CBB Big DNA Kit (Circulomics) following the manufacturer's instructions and eluted in EB buffer (Qiagen). The sequencing libraries were prepared using the ligation sequencing kit SQK-LSK109 from Oxford Nanopore Technologies (ONT). Briefly, 4.0 μg DNA was DNA-repaired and DNA-end-repaired using NEBNext FFPE DNA Repair Mix (NEB) and the NEBNext UltraII End Repair/dA-Tailing Module (NEB). Then, sequencing adaptor ligation, purification by 0.4× AMPure XP Beads and elution in Elution Buffer (SQK-LSK109) was accomplished. The sequencing runs were performed on a GridION Mk1 (ONT) using a Flowcell R9.4.1 FLO-MIN106D (ONT) and the sequencing data were collected for 110 hr. The quality parameters of the sequencing runs were monitored by the MinKNOW platform version 4.1.2 in real time and base-called with GUPPY version 4.2.3.

2.2.2 | Short-read whole genome sequencing

The short-insert paired-end libraries for whole genome sequencing (WGS) were prepared from DNA of the same female used for long-read sequencing with a PCR-free protocol using KAPA HyperPrep kit (Roche) with some modifications. In short, 1.0 μg of genomic DNA was sheared on a Covaris LE220-Plus (Covaris) and size-selected for the fragment size of 220–550 bp with AMPure XP beads (Agencourt, Beckman Coulter). The genomic DNA fragments were then end-repaired and adenylated. Next, compatible adaptors for Illumina platforms with unique dual indexes including unique molecular identifiers (Integrated DNA Technologies) were ligated. The libraries were quality controlled on an Agilent 2100 Bioanalyser with the DNA 7500 assay (Agilent) for size and quantified by Kapa Library Quantification Kit for Illumina platforms (Roche).

2.2.3 | RNA-Seq

Two different projects fed RNA data into our study, which included mRNA and small RNA sequencing. In the first project RNA-Seq was performed on brain, liver and head kidney using pools of two females for each tissue. In the second one, RNA-Seq and small RNA-Seq were was performed on vertebral bone, muscle, fin and 31 days after hatching (dah) postlarvae using several juveniles (123 dah) or postlarvae samples. Total RNA extraction was performed in both projects using the RNeasy mini kit (Qiagen) with DNase treatment. RNA quantity and quality were evaluated with the Qubit RNA BR Assay kit (Thermo Fisher Scientific), and RNA integrity was estimated by using an RNA 6000 Nano Bioanalyser 2100 Assay (Agilent). Next, single individuals or equimolar RNA pools of several individuals were used for library construction of each tissue after evaluation of individual RNA extractions.

The RNA-Seq libraries of the first project were prepared with a KAPA Stranded mRNA-Seq Illumina Platforms Kit (Roche) following the manufacturer's recommendations. Briefly, 500 ng of total RNA was used for the poly-A fraction enrichment with oligo-dT magnetic beads, following mRNA fragmentation. Strand specificity was achieved during the second strand synthesis performed in the presence of dUTP instead of dTTP. Blunt-ended double stranded cDNA was 3′ adenylated before Illumina platform-compatible adaptors with unique dual indexes and unique molecular identifiers (Integrated DNA Technologies) were ligated. The ligation product was enriched with 15 PCR cycles and the final library was validated on an Agilent 2100 Bioanalyser with the DNA 7500 assay.

The short-read WGS and RNA-Seq libraries were sequenced on a NovaSeq 6000 (Illumina) in paired-end mode, with a read length of 151 bp for the WGS and 100 bp for the RNA-Seq following the manufacturer's protocol for dual indexing. Image analysis, base calling and quality scoring of the run were done using the manufacturer's

software Real Time Analysis (RTA 3.4.4) and followed by generation of FASTQ sequence files.

A similar methodology was applied for the second RNA-Seq project with minor technical modifications: total RNA was extracted using TRIzol Reagent (Life Technologies) and the quantity and purity of RNA were determined in a NanoDrop ND-1000 spectrophotometer (NanoDrop Technologies). Samples of total RNA of the different stages and tissues were delivered to Novogene-Europe for constructing poly-A-enriched mRNA and small RNA libraries to be sequenced in 150-bp pair-end and 50-bp single-end mode, respectively, using an Illumina NovaSeq 6000 platform.

2.3 | Genome assembly

Before assembly, reads were preprocessed as follows: the Illumina reads were trimmed using TRIM-GALORE version 0.6.6 (with options *--gzip -q 20 --paired --retain_unpaired*) (https://www.bioinformatics.babraham.ac.uk/projects/trim_galore/) and the nanopore reads were filtered using FILTLONG version 0.2.0 (with options *--min_length* 5000 *--target_bases* 40,000,000,000) (FiltLong: https://github.com/rrwick/Filtlong). The filtering of nanopore data ensured having reads of at least 5 kb while optimizing for both length and higher mean base qualities, keeping 40 Gb (~65× coverage).

We assembled the filtered ONT reads with NEXTDENOVO version 2.4.0 (https://github.com/Nextomics/NextDenovo) applying the options: minimap2_options_raw=−x ava-ont, minimap2_options_cns=−x ava-ont -k17 −w17 and seed_cutoff = 10 k. The resulting contigs were polished with NEXTPOLISH version 1.3.1 (Hu et al., 2020) using two rounds of long-read polishing and two rounds of short-read polishing. This assembly (fSolSen1.1) was evaluated with BUSCO version 5.4.0 (Simão et al., 2015) using actinopterygii_odb10 in genome mode, and MERQURY version 1.1 (Rhie et al., 2020) for consensus quality (QV) and k-mer completeness. Note that the MERQURY QV is computed as the Phred quality score treating E as the base error probability QV = $-10 \times \log_{10} E$. Finally, to compute the contiguity we used our in-house script Nseries.pl (https://github.com/cnag-aat/assembly_pipeline/blob/v2.0.0/scripts/Nseries.pl).

2.4 | Genome annotation

Repeats present in the fSolSen1 genome assembly were annotated with REPEATMASKER version 4-0-7 (http://www.repeatmasker.org) using the custom repeat library available for *Danio rerio*. Moreover, a new repeat library specific for our assembly was made with REPEATMODELER version 1.0.11. After excluding those repeats that were part of repetitive protein families (performing a BLAST search against UniProt) from the resulting library, REPEATMASKER was run again with this new library in order to annotate the specific repeats.

The gene annotation of the assembly was obtained by combining transcript alignments, protein alignments and ab initio gene predictions. First, RNA-Seq reads obtained from several tissues and developmental stages, either sequenced specifically in this study (brain, liver, bone, muscle, head kidney, fin and 31 dah postlarvae) or existing in public databases, were aligned to the genome with STAR (Dobin et al., 2013) (version 2.7.2a). Transcript models were subsequently generated using STRINGTIE (Pertea et al., 2015) (version 2.0.1) on each BAM file and then all the models produced were combined using TACO version 0.6.2. PASA assemblies were produced with PASA (Haas et al., 2008) (version 2.4.1) and the TRANSDECODER program, which is part of the PASA package, was run on the PASA assemblies to detect coding regions in the transcripts. Second, the complete *D. rerio*, *Scophthalmus maximus* and *Cynoglossus semilaevis* proteomes were downloaded from UniProt in April 2020 and aligned to the genome using SPALN (Slater & Birney, 2005) (version 2.4.03). Ab initio gene predictions were performed on the repeat-masked fSolSen1 assembly with three different programs: GENEID (Parra et al., 2000) version 1.4, AUGUSTUS (Stanke et al., 2006) version 3.3.4 and GENEMARK-ES (Lomsadze et al., 2014) version 2.3e with and without incorporating evidence from the RNA-Seq data. The gene predictors were run with trained parameters for human, except GENEMARK that runs in a self-trained manner. Finally, all the data were combined into consensus CDS models using EVIDENCEMODELER-1.1.1 (EVM, Haas et al., 2008). Additionally, untranslated regions (UTRs) were identified, and alternative splicing forms annotated through two rounds of PASA annotation updates. Functional annotation was performed on the annotated proteins with BLAST2GO (Conesa et al., 2005). First, a DIAMOND blastp (Buchfink et al., 2021) search was made against the nr (last accessed May 2021) and Uniprot (last accessed August 2021) databases. Then, INTERPROSCAN (Jones et al., 2014) was run to detect protein domains on the annotated proteins. All these data were combined by BLAST2GO, which produced the final functional annotation results.

The noncoding RNA annotation required several steps. First, those expressed transcripts that had been assembled by PASA but that had not been annotated as protein-coding genes were tagged as long-noncoding (lnc)RNAs. The reason for this step is that it helps to have putative lncRNAs annotated before using annotation for downstream analysis. However, due to a lack of lncRNA conservation between species, no function was assigned to these lncRNA genes. Moreover, in order to remove false positives, transcripts overlapping with other protein-coding genes or repeats were not included in the lncRNA annotation. Finally, only transcripts longer than 200 bp were considered lncRNAs.

We also used small RNA data from vertebral bone, muscle, fin and 31 dah postlarvae to facilitate their annotation in the *S. senegalensis* genome. The corresponding reads were aligned with STAR (Dobin et al., 2013) (version 2.7.2a) with parameters (-outFilterMultimapNmax 25 --alignIntronMax 1 --alignMatesGapMax 1,000,000 --outFilterMismatchNoverLmax 0.05 --outFilterMatchNmin 16 --outFilterScoreMinOverLread 0 --outFilterMatchNminOverLread 0). The resulting mappings were processed to produce the annotation of small noncoding (snc)RNAs. First, TACO was run to assemble the reads into transcripts. Transcripts overlapping exons from the protein-coding or lncRNA annotations

were removed from the set of sncRNAs. Finally, the program CMSEARCH (Cui et al., 2016) (version 1.1.4) that includes the embedded tool INFERNAL (Nawrocki & Eddy, 2013) was run on the sncRNAs against the RFAM (Nawrocki et al., 2015) database of RNA families (version 14.6) in order to annotate products of those genes.

The final noncoding annotation contains the lncRNAs and sncRNAs. The resulting transcripts were clustered into genes using shared splice sites or substantial sequence overlap as criteria for designation as the same gene.

2.5 | Genetic map construction and genome reassembly

Six *S. senegalensis* breeders, three males and three females, were used for producing three full-sib families using in vitro fertilizations as described for the proof-of-concept experiment by Ramos-Júdez et al. (2021). Briefly, females were selected by maturity status and induced to ovulate with an injection of 5 $\mu g\,kg^{-1}$ of GnRHa (Sigma code L4513, Sigma), whilst no hormones were used on males. Gametes were extracted from females and males using gentle abdominal pressure, fertilized (1 male ×1 female) and incubated in 30-L incubators. Larvae were randomly sampled from the incubators and placed in 70% ethanol 8 days post-fertilization (dpf). All this work was performed at the IRTA Sant Carles de la Rápita Center (Catalonia, Spain).

Library preparation for single nucleotide polymorphism (SNP) calling and genotyping followed the 2b-RAD protocol (Wang et al., 2012) with slight modifications (Maroso et al., 2018). The use of this methodology for genotyping was successfully applied for high-density genetic map construction in other flatfish such as *S. maximus* (Maroso et al., 2018). Briefly, DNA samples were adjusted to 80 $ng\,\mu l^{-1}$ and digested using the IIb type restriction enzyme *Alf*I (Thermo Fisher). Specific adaptors and individual sample barcodes were ligated and the resulting fragments were amplified. After PCR purification, samples were quantified and equimolarly pooled. The pools were sequenced on a NextSeq 500 Illumina sequencer in the FISABIO facilities (Valencia, Spain). A total of 81, 77 and 71 offspring from the three full-sib families founded (Fam1, Fam2 and Fam3, respectively) were evenly mixed within each family and sequenced in three independent runs with parents also included at double concentration.

Demultiplexed reads according to the sample barcodes were first trimmed to 36 nucleotides and a custom perl script was used to remove reads without the *Alf*I recognition site in the correct position (https://github.com/abhortas/USC-RAD-seq-scripts). Then, reads were processed using the *process_radtags* module in STACKS version 2.0 (Catchen et al., 2013), removing reads with uncalled nucleotides or a mean quality score below 20 in a sliding window of 9 nucleotides. BOWTIE 1.1.2 (Langmead et al., 2009) was used to align the filtered reads against the assembled genome (see above), allowing a maximum of three mismatches and a unique valid alignment. Finally, the output files were used to feed the *gstacks* module in STACKS, using the *marukilow* model to call variants and genotypes.

To build the genetic map, SNPs with extreme deviations from Mendelian segregation (chi-square; $p < .001$) were removed, and only informative SNPs genotyped in at least 60% offspring were used. The *grouping* function of JOINMAP 4.1 (Stam, 1993) was used to build linkage groups (LGs), based on an increasing series of LOD scores from 7.0 to 10.0 to accommodate to the 21 chromosomes (C) of the *S. senegalensis* karyotype (Vega et al., 2002). Marker ordering was performed using the maximum likelihood (ML) algorithm with default parameters with the Kosambi mapping function used to compute centi-Morgan (cM) map distances. Consensus maps were built using MERGEMAP (Wu et al., 2011) and visualized with MAPCHART 2.3 (Voorrips, 2002) and CIRCOS software (Krzywinski et al., 2009).

CHROMONOMER 1.13 (Catchen et al., 2020) was used with default parameters to anchor and orient the contigs of the genome to the genetic map. CHROMONOMER assigns each scaffold to an LG and find the maximum set of nonconflicting markers to assign a forward or reverse orientation to the contig. Further, the correspondence between genetic map and contigs enabled the manual curation of original contigs that mapped to different LGs. This occurred with the longest contig (see Results), which was split into two fragments at a specific position following the method of Maroso et al. (2018). Briefly, we first considered the middle of the gap between the two markers that flanked the two fragments mapping on different LGs according to CHROMONOMER information, and then refined the breakpoint by comparing the sequence between both markers with orthologous regions of other flatfish chromosome-level genomes available in Ensembl. The program RIDEOGRAM was used to visualize the correspondence between genome contigs and chromosomes (Hao et al., 2020).

2.6 | Cytogenetic map and mapping integration

The BAC clones used for mapping came from an *S. senegalensis* BAC library including 29,184 clones (García-Cegarra et al., 2013). To establish the correspondence between LGs/genome scaffolds and the chromosomes for mapping integration, 141 BAC clones previously positioned on chromosomes using BAC-FISH (bacterial artificial chromosome fluorescence in situ hybridization) were located in the 21 scaffolds of the genome by a megablast search tool from the blast algorithm (Altschul et al., 1990) using the following parameters: Evalue < E-20; max_hsps = 10; sequence overlap >5 kb. Alignments were visualized with the Integrative Genomics Viewer (IGV) program (Robinson et al., 2017) and manually explored.

2.7 | Sex determining (SD) gene candidates

DNA extracted from fin-clips of six adult males and six adult females was resequenced using 150-bp paired-end reads on an Illumina NovaSeq 6000 System to 20× coverage in the Centre Nacional d'Anàlisi Genòmica (CNAG, Barcelona, Spain) Platform following the outlined short-read WGS protocol. The high-throughput SNP

screening of the genome was expected to identify a narrow sex-associated region to be further validated on specific markers in a broad sample of males and females. The reads were filtered using FASTP version 0.19.7 (Chen et al., 2018), trimming bases with Phred quality <15 and reads with length <30 bp, and then each sample was aligned independently against the newly assembled reference *S. senegalensis* genome using Burrows-Wheeler Aligner version 0.7.17 (Li & Durbin, 2009) with default parameters. A broad SNP data set was identified and genotyped in those six males and six females using SAMTOOLS version 1.10 (Li et al., 2009) and SNPs showing quality scores below 20 were removed. This SNP data set was used to estimate the relative component of genetic differentiation between males and females (F_{ST}) and the intrasex fixation index (F_{IS}) across the whole genome using GENEPOP 4.7.5 (Raymond & Rousset, 1995). F_{ST} and F_{IS} values were averaged over 50 consecutive SNPs and explored using sliding windows across each chromosome of the genome to look for deviation from the null hypothesis (F_{ST} and $F_{IS} = 0$).

2.8 | Developing a tool for sexing

As shown in the Results, *fshr* was the most consistent SD candidate gene. It included a large number of diagnostic markers across its whole length, homozygous in females and heterozygous in males, which agrees with the XX/XY system reported for *S. senegalensis* (Molina-Luzón et al., 2015). Several of these markers were used to develop a molecular tool to identify sex using a noninvasive method (e.g., from a fin-clip). This tool was valuable to assess gene expression across gonad development from the undifferentiated germinal primordium, especially at those stages where the gonad was still undifferentiated (see below). A SNaPshot assay used for SNP genotyping was developed for three diagnostic markers, chosen by their technical feasibility (i.e., with no other polymorphism within ±100 bp from the SNP), according to the resequencing information of six males and six females, and using three different regions (exons 12 and 14, and 3′UTR). The SNaPshot assay consists of two consecutive reactions; the first step involves the PCR amplification of the region where the target SNP is located and the second a minisequencing reaction from a primer adjacent to the SNP site using dideoxy nucleotides. Thus, two flanking PCR primers and one internal primer adjacent to the variable site were designed for genotyping each SNP using PRIMER 3 software (Rozen & Skaletsky, 2000) taking flanking sequences from our assembled genome. SNaPshot products were separated in an ABI 3730xl Genetic Analyser (Applied Biosystems) and results were analysed with GENEMAPPER 4.0 software (Applied Biosystems). PCR was performed on a Verity 96-Well Thermal Cycler (Applied Biosystems) as follows: initial denaturation at 95°C for 5 min, 30 cycles of denaturation at 94°C for 45 s, annealing temperature at 58°C for 50 s and extension at 72°C for 50 s; a final extension step was done at 72°C for 10 min. Subsequently, 1 μl of the PCR product was purified by incubation with 0.5 μl illustra ExoProStar 1-STEP Kit at 37°C for 15 min followed by 85°C for 15 min to eliminate unincorporated primers and dNTPs. The SNaPshot mini-sequencing reaction was carried out using the SNaPshot Multiplex Kit (Applied Biosystems) in an ABI Prism 3730xl DNA sequencer. For each reaction, 1.5 μl of purified PCR product, 0.5 μl (2 μM) of the internal primer and 2 μl of SNaPshot Multiplex Ready Reaction Mix were used in a final volume of 5 μl. The reaction profile consisted of initial denaturation at 96°C for 1 min, 30 cycles at 96°C for 10 s, 55°C for 5 s and 60°C for 30 s. The extension product was incubated with 1 μl of shrimp alkaline phosphatase at 37°C for 60 min followed by 85°C for 15 min to remove unincorporated dideoxinucleotides (ddNTPs) after thermal cycling. The three sex-associated candidate SNPs were checked in a small sample of adult males and females for SNaPshot performance, and then, the best one was validated in a large sample of 48 male and 48 female *S. senegalensis* adults provided by a farm company, where they are routinely used for breeding. Additionally, 38 individuals where information for gonadal sex and genotyping for the sex marker was available were also used to check for the association between genotypic and the phenotypic sex, thus totalling 134 individuals: 12 whole genome resequenced individuals (six males and six females); six individuals used for anatomy/histology analysis (126 dpf); and 10 juveniles and 10 fry (126 dpf) from the qPCR/RNA-Seq assays.

2.9 | Gonad differentiation: Histological evaluation

Three fish per sex and stage were collected at 84, 98 and 126 dpf, juveniles (315 dpf) and mature adults (810 dpf) at Stolt Sea Farm SL facilities and killed by decapitation. All fish were maintained at the same standard temperature, air-flow and feeding conditions of the usual production protocol of the company until being killed. Gonads were dissected fresh for macroscopic evaluation and classified as testes or ovaries by visual inspection in juveniles and adults. At the three initial stages, the molecular tool outlined before was used for sexing. Then, the gonads were fixed by immersion in 4% paraformaldehyde and later embedded in paraffin wax to be cut into sagittal sections 3–6 μm and stained with haematoxylin-eosin for optical microscopy evaluation. Experimental procedures for the use of farm animals were carried out following the regulations of the University of Santiago de Compostela and Stolt Sea Farm SA company and the Guidelines of the European Union Council (86/609/EU).

2.10 | Gonad differentiation: Gene expression

Gene expression of the *fshr* gene along with several marker genes for the initial stages of gonadal differentiation were evaluated through qPCR on five male and five female gonads at the five developmental stages considered: 84, 98 and 126 dpf, juveniles and adults. Stages were chosen considering histological data on *S. senegalensis* (this study; Viñas et al., 2013) and previous information in *S. maximus*, a species with a similar gonadal developmental pattern (Robledo et al., 2015). RNA extraction was performed using the RNeasy mini kit (Qiagen) with DNase treatment, and RNA quality and quantity were

evaluated in a Bioanalyser (Bonsai Technologies) and in a NanoDrop ND-1000 spectrophotometer (NanoDrop Technologies), respectively. Primers for qPCR of the candidate gene (*fshr*, see Results), and for ovary (*cyp19a1*, aromatase) and testes (*amh*, anti-müllerian hormone; *sox9*, SRY-Box Transcription Factor 9) markers (Robledo et al., 2015), along with those related to germinal cell proliferation (*gsdf*, gonadal soma-derived factor, and *vasa*, ATP-dependent RNA helicase) were designed using the PRIMER 3 software using the annotation of the *S. senegalensis* genome presented here. Reactions were performed using a qPCR Master Mix Plus for SYBR Green I No ROX (Eurogenetec) following the manufacturer's instructions, and qPCR was carried out on an MX3005P (Agilent Technologies). Analyses were performed using the MXPRO software (Agilent). The ribosomal protein S4 (*rps4*) and L17 (*rpl17*) genes, and ubiquitin (*ubq*), previously validated for qPCR in turbot gonads by Robledo et al. (2014), were used as reference genes. Two technical replicates were included for each sample. The ΔΔCT method (Kubista et al., 2007) was used to estimate gene expression; briefly, Ct values were normalized using the reference genes, log-transformed and finally mean-centred to obtain mean-centred fold change values which were used for statistical analysis. An unpaired Student's *t* test was used to determine significant differences between sex at each stage.

Additionally, data from an ongoing RNA-Seq study on gonad differentiation were used to validate diagnostic SNPs on the exons of the SD candidate *fshr* gene and, in particular, to estimate gene expression of the X-linked and Y-linked alleles (see Results). Samples of total RNA were delivered to Novogene-Europe for constructing poly-A-enriched mRNA to be sequenced in 150-bp pair-end format using an Illumina NovaSeq 6000 platform. Raw RNA-Seq reads were filtered using FASTP version 0.19.7 (Chen et al., 2018), trimming bases with Phred quality <15 and reads with length < 30 bp, and then each sample was aligned independently against the *S. senegalensis* genome using STAR version 2.7.9a (Dobin et al., 2013) using default parameters. SNPs were identified using MPILEUP and the variant calling command of BCFTOOLS (Li, 2011). The resulting vcf file was used to obtain read counts corresponding to each SNP. Then, for each SNP (0: reference allele, 1: alternative allele in the *S. senegalensis* genome), homozygous females (0/0 or 1/1) and heterozygous males (0/1) were identified using a read counting ≥8 for consistent genotyping to avoid misclassification of heterozygotes as false homozygotes. Using genotyping across all exons, females (0/0, 1/1) and males (0/1) were consistently identified, confirming the gonadal sex, when gonads were histologically differentiated or when the genetic sex was obtained using the molecular tool. Only those individuals with consistent genotyping at ≥33% diagnostic SNPs of the *fshr* gene were considered for further analysis. Then, the number of reads of the X-linked allele (0 when females were 0/0 or 1 when females were 1/1) and of the Y-linked allele (the opposite: 1 when females were 0/0, or 0 when females were 1/1) were counted in each male for all the stages evaluated. Reads of the X-linked and of the Y-linked alleles were pooled across all exons for each individual and normalized per million reads to be compared at each stage and across all stages. Nonparametric paired-samples Wilcoxon tests were used to compare X-linked and Y-linked normalized counts across all stages and at each stage.

2.11 | Protein structure modelling on X- and Y-linked allelic variants of *fshr*: Comparison with other Pleuronectiformes

We evaluated 3D protein structure models to infer potential functional differences between X- and Y-linked allelic variants of FSHR. To find potential template structures for modelling, a specific PSI-BLAST sequence search in the PDB was performed (https://blast.ncbi.nlm.nih.gov/Blast.cgi) (Altschul et al., 1990). The identified template structure showed unresolved regions which encompass nonsynonymous mutations analysed in the present study. Two different strategies for modelling were undertaken: I-TASSER (Zhang, 2008) and RoseTTAfold (Baek et al., 2021). I-TASSER is a metaserver that automatically employs 10 threading algorithms in combination with ab initio modelling to build the tertiary structure of a protein as well as replica-exchange Monte Carlo dynamics simulations for atomic-level refinement. For comparison, a deep learning-based modelling method, RoseTTAFold (https://robetta.bakerlab.org), was also applied. The putative presence of intrinsically disordered regions in the proteins was investigated by the following predictors: PONDR (Romero et al., 2001), DISOPRED (Jones & Cozzetto, 2015), IUPRED3 (Erdös et al., 2021) and PRDOS (Ishida & Kinoshita, 2007).

To compare the evolutionary rate of the X- and Y-linked alleles of the follicule stimulating hormone receptor (*fshr*) gene (SD candidate, see Results) from the putative undifferentiated ancestor, the sequences of their encoded protein variants were compared to those from other flatfish with confident annotation and chromosome-level assemblies available in public databases. We took information of the orthogroup corresponding to *fshr* from the analysis performed by de la Herrán et al. (2022) on *S. senegalensis*, *Hippoglossus hippoglossus*, *H. stenolepis*, *Paralychthys olivaceous*, *S. maximus* and *C. semilaevis*, using *D. rerio* as an outgroup. The protein sequence corresponding to *S. senegalensis* in that analysis was replaced by the protein sequences encoded by the X- and Y-linked alleles and, then, a phylogenetic tree was constructed after whole sequence alignment using CLUSTAL W2 (Larkin et al., 2007). Phylogenetic reconstructions were performed using the function "build" of ETE3 3.1.2 (Huerta-Cepas et al., 2016) and an ML tree was inferred using PHYML version 20,160,115, where branch supports were computed out of 100 bootstrapped trees (Guindon et al., 2010).

3 | RESULTS

3.1 | Genome assembly and annotation

The initial assembly comprised 82 contigs with an N50 of 23.4 Mb (sizes ranging from 0.3 to 30.1 Mb) for a total assembly size of 614 Mb (Table S1). A high-density genetic map was used to place

51 contigs, representing 98.9% of the whole assembly (607.9 Mb), into the 21 chromosomes of the *Solea senegalensis* haploid karyotype ($n = 21$; Vega et al., 2002) (see below). This assembly is highly contiguous (contig N50: 23.4 Mb, scaffold N50: 29.0 Mb) and displays high consensus quality (QV = 43.17, which corresponds with a sequence accuracy of 99.995%), and gene (98.4% Complete BUSCO genes) and k-mer (98.18%) completeness (Table S1). Consistent with the low percentage of duplicated BUSCOs (1.0%), the k-mer spectra (Figure S1) did not reveal any evidence of artificial duplications. The repetitive peak observed at 360× probably corresponds to true long repetitive regions captured by the nanopore reads (Figure S1).

Repetitive sequences made up to 8.2% of the *S. senegalensis* genome (Table S2). These consisted of three main categories: simple repeats (2.8%), low-complexity motifs (0.3%) and transposable elements (TEs) (4.7%). The TE-derived fraction was very similar to that found in other high-quality flatfish genome assemblies, 5.8% in *Cynoglossus semilaevis* (Chen et al., 2014) and 5.0% in *S. maximus* (Figueras et al., 2016), respectively. The *S. senegalensis* genome displayed a higher TE proportion than *Tetraodon nigroviridis* and *Fugu rubripes* (<3%), but much lower than that observed in other fish such as *Danio rerio* (>40%) (Gao et al., 2016).

In total, 24,264 protein-coding genes producing 40,511 transcripts (1.67 transcripts per gene) and coding for 37,259 unique protein products were annotated (Table S3). We were able to assign functional labels to 85% of the annotated proteins. The annotated transcripts contained 12.79 exons on average, with 95.5% of them being multi-exonic. The median length of the protein-coding genes present in this annotation was 7566 bp, a value that is consistent with the annotation of the *S. senegalensis* genome assembly published by Guerrero-Cózar et al (7368 bp). In addition, 52,888 candidate noncoding RNAs were annotated (6871 lncRNAs and 46,017 sncRNAs).

3.2 | Genetic map construction and genome scaffolding

2b-RAD-seq was used for genotyping three full-sib families, consisting of 81 (Fam1), 77 (Fam2) and 71 offspring (Fam3) and the six corresponding parents (Table S4). The *gstacks* module rendered a total of 156,981 loci, 35,441 of them containing at least one SNP, and 16,890, 15,457 and 16,715 SNPs were retained for map construction in Fam1, Fam2 and Fam3, respectively. These represent 29,126 unique SNPs (47.5 SNPs per Mb), with 4889 SNPs shared among the three families.

Separate male and female genetic maps were built in each family. A LOD score of 9.0 was applied to match with the $n = 21$ chromosomes of the species. The average number of markers per LG across all maps was 434 (range: 93–694) (Tables S5 and S6). Female maps were slightly longer than male maps (average F vs. M recombination ratio of 1.1:1). Shared markers across families were used to build the female, male and species consensus maps. The final species consensus map included 28,838 markers across 21 LGs spanning 40,704.47 cM (Figure S2), a length exceeding that expected based on genome size. This artefactual elongation is related to the limitations of the software to accommodate such a number of markers in a consensus framework from several individual maps, as previously reported (Maroso et al., 2018).

Using CHROMONOMER, we anchored and oriented 51 of the initial 82 genome contigs to the 21 LGs of the consensus map (Table S7). Those 51 contigs assembled represented 98.9% of the 614 Mb of the genome placed into the 21 chromosomes of the *S. senegalensis* karyotype. Only one contig was split into two fragments assigned to LG6 and LG9 (Figure 1). After this anchoring step supported by the genetic map, the new genome significantly improved upon the 90.0% reported by Guerrero-Cózar et al. (2021) and it was similar to other flatfish genomes recently assembled (Table S8). The new assembly showed a one-to-one correspondence at the chromosome level with the previous version of Guerrero-Cózar et al. (2021) (Figure S3; Table S5). However, the substantial fragmentation of the previous version (1937 scaffolds vs. 82 contigs) gave rise to discrepancies related to wrong orientation of many minor contigs across most chromosomes.

3.3 | Cytogenetic map and mapping integration

A total of 141 BACs were used to anchor the LGs/scaffolds to the chromosomes of the *S. senegalensis* karyotype using previous BAC-FISH information (Table S9; Figure S4). On average 6.6 BACs per scaffold were used to establish the correspondence between the genetic, physical and cytogenetic maps (range: 4–14 BACs), thus providing a robust mapping integration (Figure 1). Ten out of 141 BACs were localized in more than one chromosome or in different locations within the same chromosome, suggesting paralogous regions (Table S9). The minor 5 S rDNA was located on C6 and C11, while signals of the major rDNA (18 S + ITS1 + 5.8) were found at C6 and C20.

3.4 | Sex determining (SD) gene candidate

Whole-genome resequencing of six males and females identified a total of 9,078,413 SNPs. A consistent pattern of genetic differentiation between males and females (average $F_{ST} = 0.304$) and significant heterozygote excess (average $F_{IS} = -0.519$) was detected at chromosome (C) 12, between 10,024,822 and 10,054,590 bp (Table S10; Figure 2).

This region included the 14 exons of the *fshr* gene and a small fragment of the 5′ end (~8012 bp) of neurexin, a long gene (~227,983 bp) involved in neuron synaptic connection (Figure 2). Out of 284 SNPs within the fshr gene, 168 were heterozygous in males and homozygous in females (sex diagnostic markers) consistent

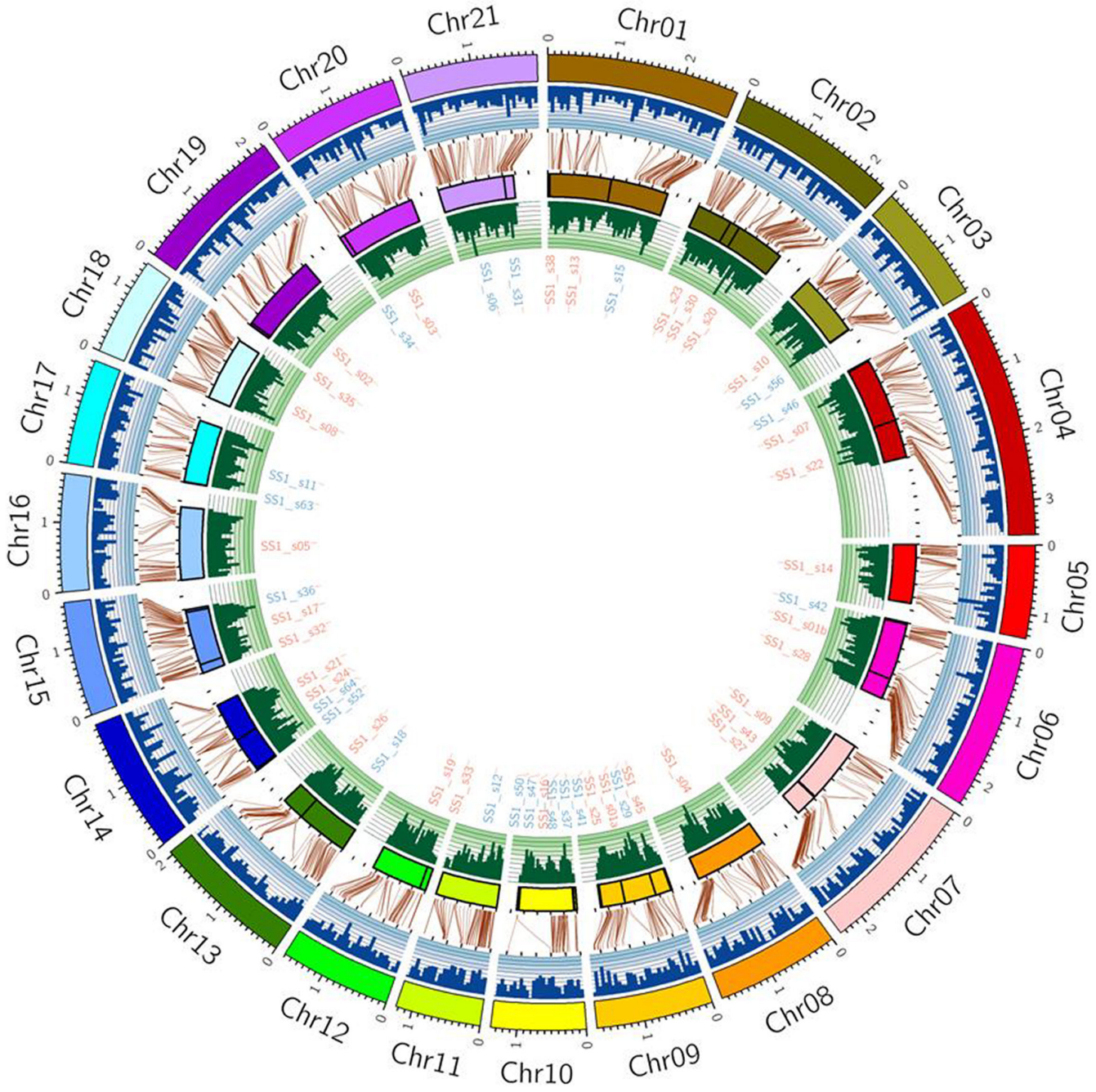

FIGURE 1 CIRCOS plot of the genome map and anchored scaffolds in *Solea senegalensis*. From outer to inner circles are represented: the 21 LGs/chromosomes (tick marks every 100 cM); histograms of the number of markers per 50 cM (in dark blue); brown lines anchoring the genome scaffolds through collinear markers in the genetic map; the 51 anchored contigs (tick marks every 5 Mb); histograms of the number of markers per Mb (in dark green); and the names of the scaffolds (in red those anchored in the reverse strand).

with the XX/XY system reported for this species (Molina-Luzón et al., 2015) (Table S11). A total of 33 diagnostic variants were located within exons of *fshr* (24 nonsynonymous), 16 of them in exon 14 (11 nonsynonymous) and five in exon 1 (three nonsynonymous). The accumulation of nonsynonymous variants might suggest the degeneration of the Y-linked *fshr* allele that could represent a nonfunctional variant, although, as shown below, this is an expressed allele involved on the SD mechanism of *S. senegalensis*.

3.5 | A molecular tool for sexing

Three diagnostic SNPs surrounded by ±100-bp conserved regions (no polymorphisms) were selected for assessing genetic sex using a SNaPshot assay. Three sets of three primers (two external and one internal) were designed (Table S12) and tested in five males and five females. One marker differentiated males and females and matched the in silico genotype expectations, and was further validated in 48

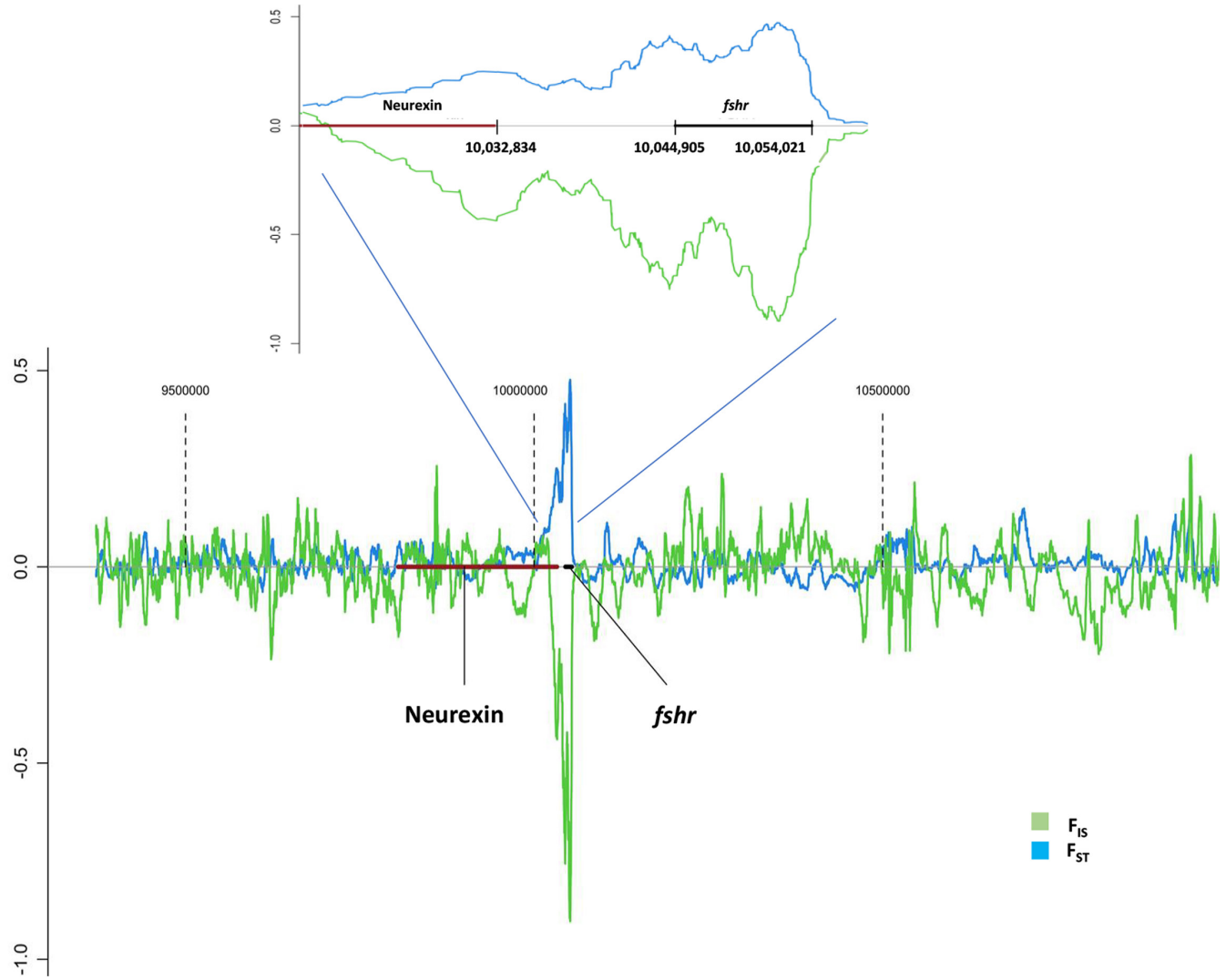

FIGURE 2 Genetic differentiation (F_{ST}) and intrapopulation fixation index (F_{IS}) between male and female populations at a section of C12 of *Solea senegalensis* (between 9372 and 11,072 kb). The enlarged region corresponds to the follicle stimulating hormone receptor gene (*fshr*).

males and 48 females from the broodstock of an *S. senegalensis* farm (SS-sex marker). In all but three fish, the genetic sex matched the phenotypic sex. These three fish were phenotypic males sexed as genetic females. Nonetheless, among a total of 134 fish with known genetic and histological sex information in this study (see Section 2), only these three males showed a discordant genotype (2.2%).

3.6 | Gonad differentiation: Gene expression analysis

We analysed gene expression of *fshr* and other relevant genes for gonadal differentiation (*amh*, *cyp19a1*, *gsdf*, *vasa* and *sox9a*), from the undifferentiated primordium until mature adults, including 84, 98 and 126 dpf, juveniles (315 dpf) and adults (810 dpf), using five males and five females at each stage, sexed either macroscopically or with the SS-sex marker (undifferentiated stages). Gonads were macroscopically identified at all stages (Figure S5) and histological observations were in accordance with previous information by Viñas et al. (2013) (Figures S6–S8).

Interestingly, the *fshr* gene was significantly overexpressed in males at all stages, despite the putative degeneration suggested for the Y-linked allele, especially in juveniles, but even at the undifferentiated 84 and 98 dpf stages (Figure 3), an observation corroborated by RNA-Seq data (Figure S9). RNA-Seq was also used to check the expression of the X-linked and the Y-linked *fshr* alleles, taking advantage of the presence of diagnostic SNPs associated with each variant. Only one male from 84 dpf did not pass the filtering criteria (≥8 reads per SNP and ≥33% genotyped exons) and was excluded for the analysis (Table S13). Interestingly, the Y-linked allele showed higher expression than the X-linked allele across all stages (paired-samples Wilcoxon test; $p = 0$) and at each stage (paired-samples Wilcoxon tests; $p < .05$), even at 84 dpf (Y-linked: 19.853 vs. X-linked: 13.944, total normalized read count), although was not significant at this stage ($p = .144$) (Figure 4; Table S13). In adults of both sexes *fshr* expression was nearly undetectable. Normalized read counts across the 14 exons of *fshr* showed a very similar profile both in males and in females, and no signs of alternative splicing were detected (Figure S10).

Additionally, marker genes of male (*sox9a* and *amh*) and female (*cyp19a1a*) gonadal differentiation and of germinal cell proliferation

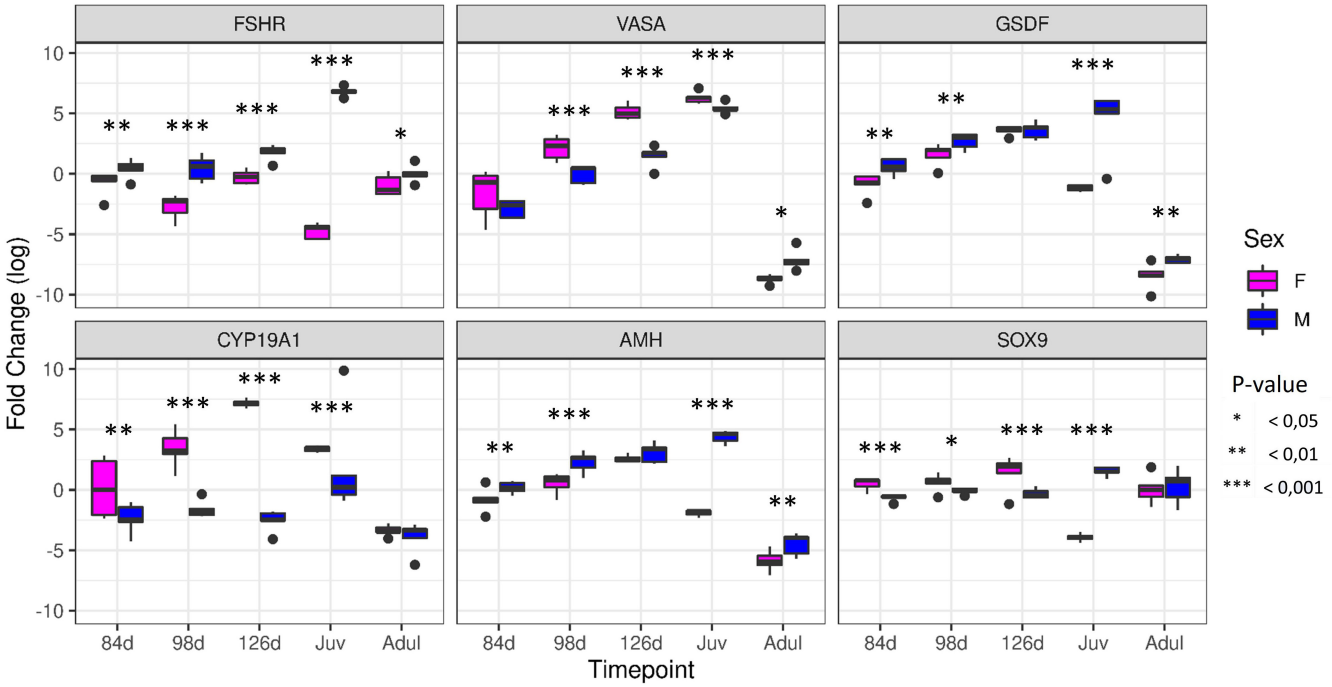

FIGURE 3 Box plots of the qPCR for the follicule stimulating hormone receptor SD gene of *Solea sonegalensis* and other key marker genes across gonad development.

FIGURE 4 Number of counts for the X- and Y-linked allelic variants of the *fshr* gene across different gonad developmental stages in *Solea senegalensis*. Five replicates were evaluated at each stage, but only those passing the filtering genotyping criteria were further analysed.

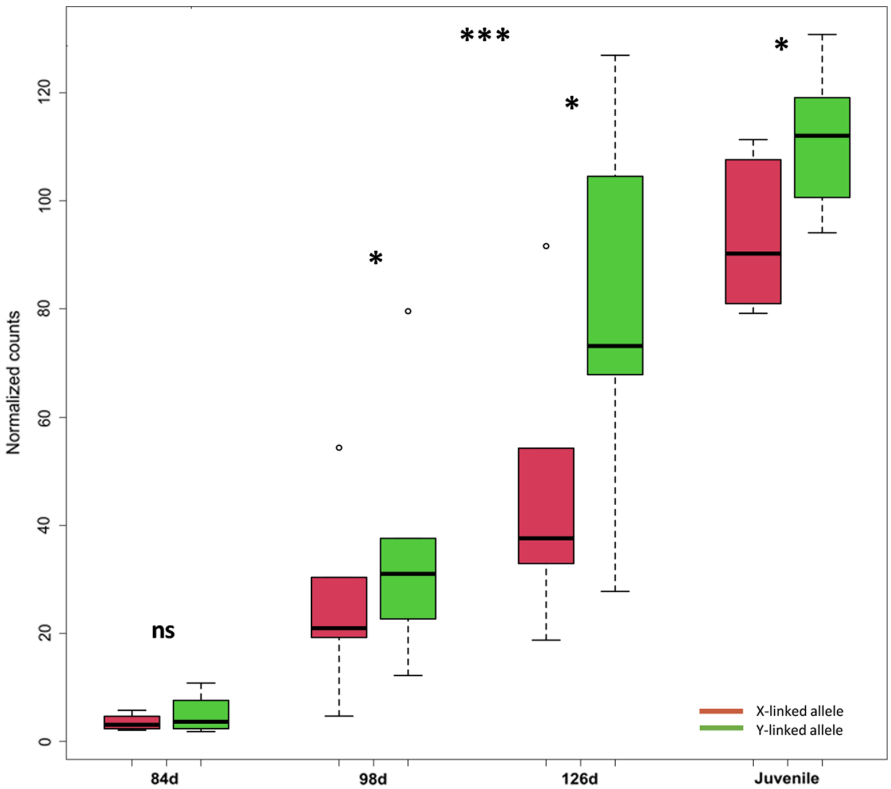

(*gsdf* and *vasa*) were evaluated by qPCR (Figure 3). While adult males and females hardly showed differential expression for the genes evaluated, juveniles showed the greatest differentiation for most of them. A progressive increase in expression was observed for sex marker genes, *cyp19a1a* in females and *amh* in males, concomitant with the two germinal cell proliferation markers, *vasa* in females and *gsdf* in males. However, *sox9a*, a marker of testis differentiation, showed higher expression in females, although not as markedly as for *cyp19a*, until the juvenile stage, when the pattern was reversed.

3.7 | 3D structure and evolutionary rate of the X- and Y-linked encoding follicule stimulating hormone receptor

The model structures obtained by RoseTTAfold were of higher quality than those generated by I-TASSER (Table S14). The models of the follicule stimulating hormone (FSH) receptor showed differences at key sites of the protein involved in the reception of the hormone and the G-coupled signal transduction domains (Figure 5). In particular, differences between the X- and Y-linked protein variants were found in the three main external domains related to the hormone binding, hairpin loop and hinge region domains (Ulloa-Aguirre et al., 2018), suggesting that proper binding of the FSH could be affected. Model structures highlighted the differences at the flexible hairpin loop with eight variants falling within the LRR extracellular domain (Figure 5a) that might alter the recognition properties of the receptor (Figure 5b). Furthermore, the E326Q variant might affect the backbone conformation, between residues 326 and 336 located at the C-terminus of the hinge region which behaves as an internal agonist unit for the receptor (Ulloa-Aguirre et al., 2018). On the internal side, related to signal transduction, the R365P replacement at IL1, adjacent to the conserved K367, L368 and F373 residues, might influence the interaction with the adapter protein APPL1; the I439L variant, close to the ERW motif, might affect activation of the G-protein (Ulloa-Aguirre et al., 2018), and amino acid replacements at IL3 (N529T, I530V and P540H) might affect the stabilization of the inactive conformation.

Furthermore, the X-linked variant of *S. senegalensis* showed higher homology with the FSHR proteins of other flatfish species (Figure S11), which indicates the divergence of the Y-linked allele from the putative ancestor, as shown by the multiple amino acid substitutions detected on the encoded protein. Together, the results suggest that the Y-linked allele could be a nonfunctional allele but expressed over the X-linked variant in males, although we cannot exclude that a neofunctionalization process is involved.

4 | DISCUSSION

4.1 | A contiguous *S. senegalensis* genome assembly

The new genome assembly of *Solea senegalensis* is among the most contiguous fish genomes assembled to date (Ramos & Antunes, 2022) and meets the standards outlined by the Earth Biogenome Project initiative (https://www.earthbiogenome.org/assembly-standards). The contiguity achieved (82 contigs; N50: 23.4 Mb) was facilitated by the small proportion of low-complexity sequences; repetitive elements only constitute 8.2% of the *S. senegalensis* genome, a similar proportion to that reported in other flatfish species (Chen et al., 2014; Figueras et al., 2016). The new *S. senegalensis* assembly comprises 21 scaffolds corresponding to the $n = 21$ chromosomes of its haploid karyotype (Vega et al., 2002) and contains 98.9% of the whole assembly, similar to other flatfish genomes recently reported (Einfeldt et al., 2021; Ferchaud et al., 2022; Jasonowicz et al., 2022; Lü et al., 2021; Martínez et al., 2021) and notably improved the previous version reported by Guerrero-Cózar et al. (2021; 90.0% assembled into chromosomes). The 21 scaffolds from our study were associated with the corresponding chromosomes of this species using previous BAC-FISH information (Ramírez et al., 2022), thus providing a sound reference for comparative genomics and for studying the genetic architecture of relevant traits, such as sex determination. The new assembly displayed one to one chromosome correspondence with the recently reported genome by Guerrero-Cózar et al. (2021), but important discordances were detected across all chromosomes, mostly related to orientation of minor scaffolds due to the higher fragmentation of the previous assembly (1937 scaffolds). This upgraded *S. senegalensis* genome allowed the identification and annotation of 24,264 protein-coding genes coding for 37,259 unique protein products (85% with functional annotation), along with 52,888 noncoding RNAs (6871 lncRNAs and 46,017 sncRNAs).

4.2 | The master SD gene of *S. senegalensis*

Guerrero-Cózar et al. (2021) reported a broad genomic region (1.4 Mb) associated with sex at SseLG18 of *S. senegalensis* (Sse C12 in our study), compatible with a nascent XX/XY system. They suggested an SD mechanism with incomplete penetrance and proposed *fshr* as the most promising master SD gene among the tens of genes existing in that region (43 in our genome), considering its role in gonad development and previous information on SD in the flathead grey mullet (Curzon et al., 2021). These authors prompted for more refined association studies and functional information to validate this gene. Here, we showed that *fshr* was the only complete gene within the region of maximum association and demonstrated the presence of a Y-linked *fshr* allelic variant (*fshry*) in *S. senegalensis*, compatible with the proposed XX/XY SD system and congruent with phenotypic sex in 97.8% of the individuals analysed. Genetic differentiation between males and females (29 kb) included only the full *fshr* gene (~9 kb), although a small fragment of the 5′ end of neurexin gene, involved in neuron synapsis, was detected at the least

FIGURE 5 Molecular modelling of the follicule stimulating hormone receptor (FSHR) encoded by X- and Y-linked alleles of the sex determining *fshr* gene of *Solea senegalensis*. (a) Structure-based sequence alignment of the two variants. Different domains and regions of the receptors are also indicated (Ulloa-Aguirre et al., 2018): ECD, leucine-rich repeat (LRR) extracellular domain; TM, transmembrane helix; EL, extracellular loop; IL, intracellular loop. (b) 3D model structures represented as coloured ribbons. Colour code is the same as for (a): grey, N-terminus and C-terminus; orange, ECD; light blue, hairpin loop; green, hinge; purple blue, TMD. Nonconserved residues between Y- and X-linked variants are shown in red.

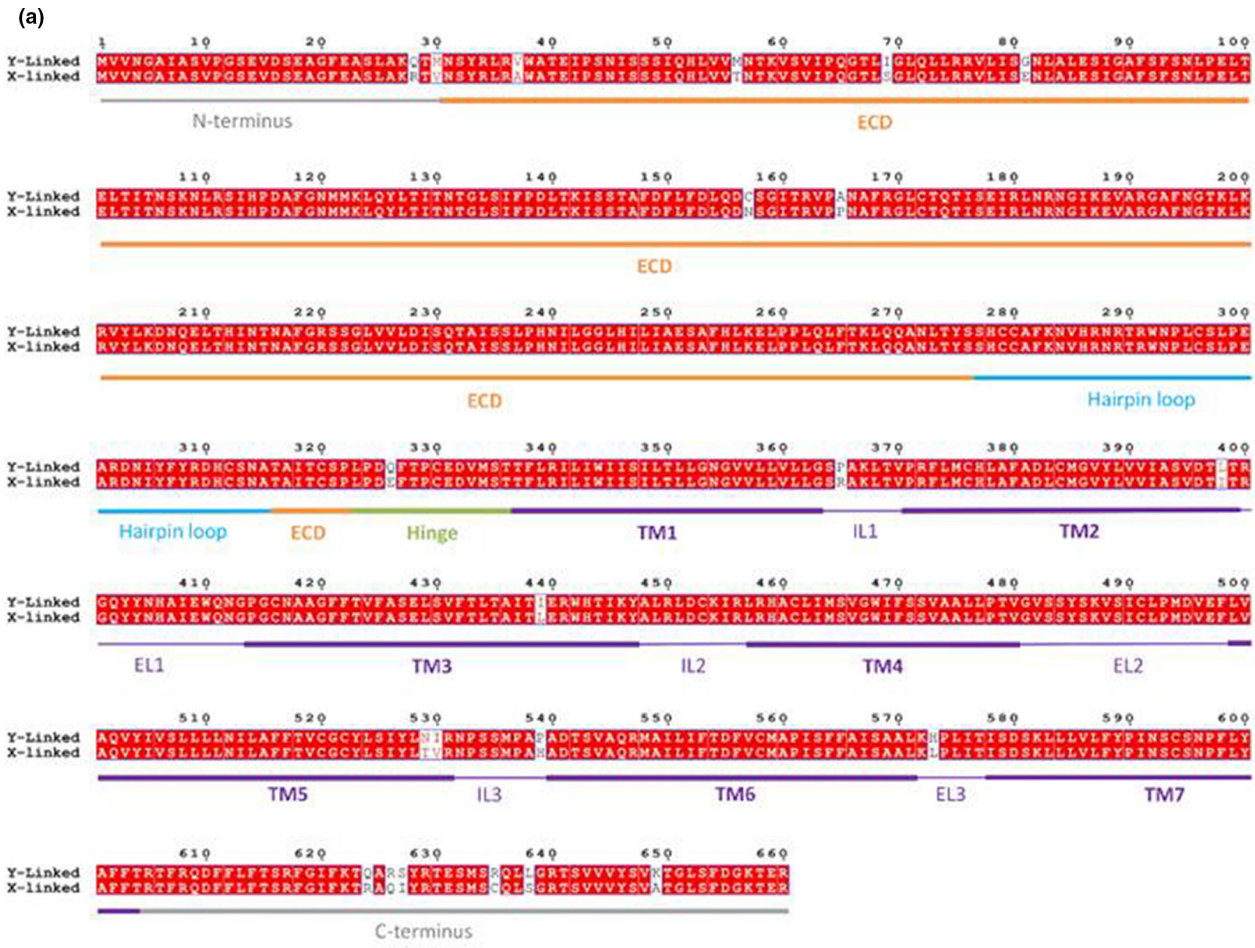

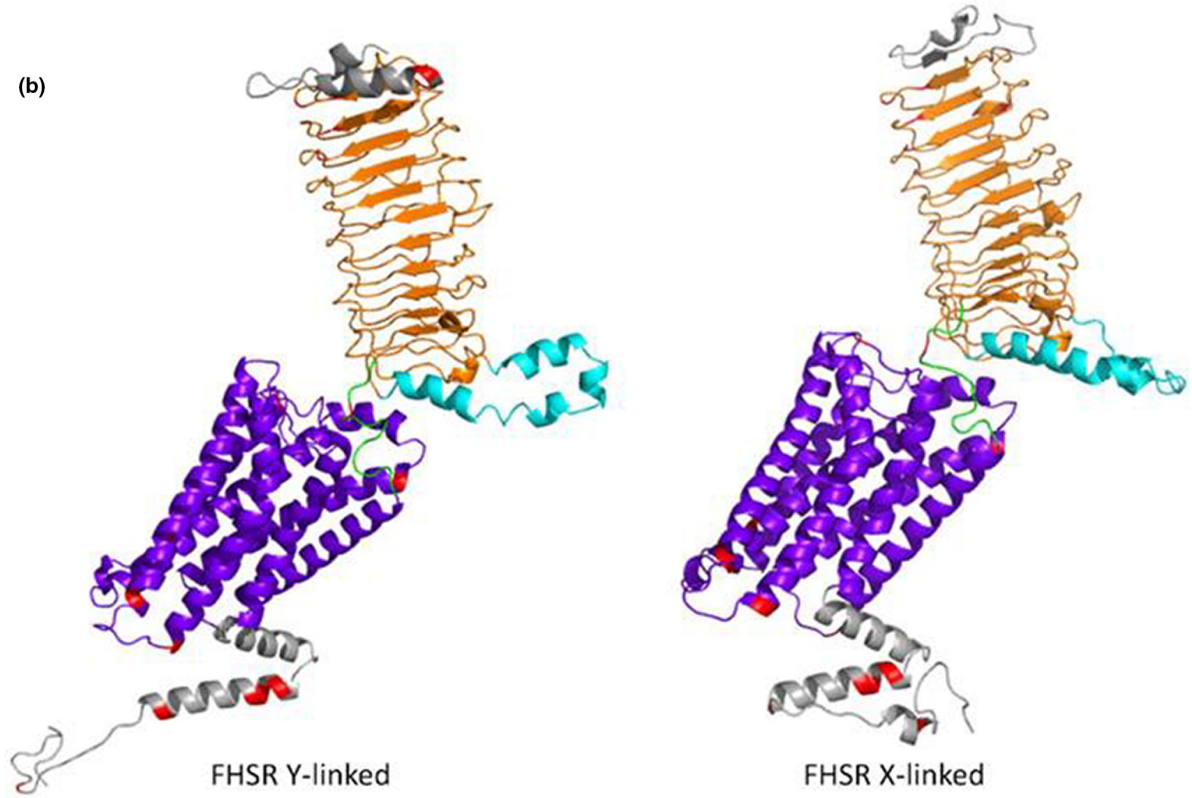

associated region. Our results strongly support an SD system mainly driven by a single gene, unlike the previous report by Guerrero-Cózar et al. (2021), who suggested a genetic SD system with incomplete penetrance involving significant environmental influence. The existence of minor genetic or environmental factors influencing SD has been usually reported, even in species with sound genetic SD systems (Martínez et al., 2014).

The *fshry* coding region showed a high number of sex diagnostic variants (33), heterozygous in males and homozygous in females, 24 of them representing nonsynonymous substitutions, which suggests a divergent function or a nonfunctional allele. This hormone receptor is G protein-coupled with seven transmembrane domains linked to an adenyl cyclase for intracellular transduction of the signal (Levavi-Sivan et al., 2010; Ulloa-Aguirre et al., 2018). Interestingly, many nonsynonymous variants were located at exon 14 and exon 1, which are part of the intracellular and extracellular domains related to signal transduction and hormone reception, respectively. In fact, 3D structure modelling supports significant differences between both FSHR isoforms at several key extracellular (hormone receptor, hairpin loop and hinge) and intracellular (internal loops, C-tail) domains. Also, the phylogenetic analysis performed within Pleuronectiformes using *Danio rerio* as an outgroup showed a divergence of the Y-linked variant from the putative ancestor, associated with the nonsynonymous substitutions detected with respect to the X-linked variant, closer to other flatfish. Nonetheless, *fshry* was not only expressed at all stages of gonadal development, but also at a higher level than the X-linked allele (*fshrx*). Moreover, we could not detect evidence of a duplication of the *fshr* gene in the male *S. senegalensis* genome assembled by Guerrero-Cózar et al. (2021), which could suggest an extra copy of *fshr* gene on the Y chromosome taking over the process of SD in the species, as reported in other fish (Matsuda et al., 2002; Hattori et al., 2012; see for review Martínez et al., 2014). Consequently, the *fshry* allele appears to be the key factor for the male fate of the undifferentiated primordium. A similar SD mechanism has been reported in flathead grey mullet, where an *fshry* allele including only two nonsynonymous variants was suggested to be responsible for the male fate of the undifferentiated primordium (Curzon et al., 2021). Considering the 24 nonsynonymous variants detected, it can be speculated that the mechanism driven by the *fshry* allele might be at a more advanced evolutionary stage in *S. senegalensis* than in flathead grey mullet, and in fact, Ferraresso et al. (2021) reported interpopulation variation of the *fshry* in flathead grey mullet, suggesting incomplete penetrance and a recent evolutionary origin of the SD gene.

The expression of *fshr* measured by both qPCR and RNA-Seq was consistently higher in males than in females starting at 84 dpf (undifferentiated gonads), and this difference increased progressively until the juvenile stage. In females, expression was very low at most stages, with the exception of 98 and 126 dpf, and in adults, where expression was nearly undetectable in both males and females. The higher expression of *fshr* in males has also been reported in other fish species such as clownfish (Kobayashi et al., 2017) and flathead grey mullet (Curzon et al., 2021), and in addition, knocking-out the *fshr* gene produced female to male sex reversal in zebrafish and medaka (Murozumi et al., 2014; Zhang et al., 2015). Furthermore, *fshr* has been suggested as the masculinization transducer of cortisol via suppression of germinal cell proliferation in response to high temperature during the sex determination period in medaka (Hayashi et al., 2010).

Analysis of *fshr* and other key genes at the initial stages of gonad differentiation in *S. senegalensis* revealed a progressive differential upregulation of *fshr*, *amh* and *gsdf* in males, while *cyp19a1* and *vasa* displayed a similar pattern in females. It should be noted that the expression of *amh*, a marker gene of testis development, also documented as a master SD gene in several fish species (or its receptor *amhr*), has been reported to be down-regulated by the FSH (Sambroni et al., 2013), so impairing its function could activate the testis pathway.

Together, our data strongly support *fshr* as the master SD gene of *S. senegalensis* and suggest that the *fshry* allele could be hampering the action of the FSH, driving the undifferentiated gonad toward testis, potentially by avoiding the suppression of *amh* activity. We hypothesize that the presence of 11 and three nonsynonymous variants in the intra- and extracellular domains of the receptor, respectively, should affect the transduction signal of *fshr*, thus blocking FSH signalling. Also, the FSHRy protein could alter trafficking of the FSH receptors in the endoplasmic reticulum, impeding their final integration in the cell membrane, and thus hampering FSH function, as reported in humans (Ulloa-Aguirre et al., 2018; Zariñán et al., 2010). Alternatively, neofunctionalization of *fshry* could be another explanation, but additional data would be necessary to understand how it could be involved in the testis triggering pathway.

4.3 | Diversification of the SD gene in Pleuronectiformes

Consistent chromosome orthology has been recently reported within flatfishes taking advantage of their chromosome-level genome assemblies facilitated by their compact genomes (de la Herrán et al., 2022; Jasonowicz et al., 2022; Lü et al., 2021; Martínez et al., 2021). According to this information, the SD gene-bearing chromosome of *S. senegalensis*, Sse C12, would not be orthologous to any other consistently proven SD chromosome in flatfish species. The low differentiated Z and W chromosomes of *Cynoglossus semilaevis* (tongue sole, Chen et al., 2014), as recently reported when compared to *Scophthalmus maximus* (turbot, Martínez et al., 2021), matched to a single *S. senegalensis* chromosome, Sse C6, which in turn is syntenic to the SD-Hst9 of *Hippoglossus stenolepis* (Pacific halibut, Drinan et al., 2018) (Figure S12). This reinforces the orthology of sex chromosomes of *C. semilaevis* and *H. stenolepis*, not being conserved in other flatfish (Martínez et al., 2021), although the *dmrt1* SD gene of *C. semilaevis* (Chen et al., 2014) is different from the candidate SD gene recently suggested for *H. stenolepis*, *bmpr1ba*, pertaining to the TGF-β family (Jasonowicz et al., 2022). Moreover, conserved synteny with another *S. senegalensis* autosome (Sse C5) was observed for the

H. hippoglossus (Atlantic halibut) SD chromosome, Hhi12, where *gsdf* has been identified as the most likely master gene for the XX/XY SD system in this species, recently derived from an ancestral ZZ/ZW in the sister *Hippoglossus* species, as recently reported (Edvardsen et al., 2022; Einfeldt et al., 2021). Interestingly, Sse C12 is orthologous to the *S. maximus* Sma C18, where a minor SD quantitative trait locus was identified and where sex-associated markers were detected in brill (*Sc. rhombus*), a congeneric XX/XY species of turbot (Taboada et al., 2014). Moreover, Sse C12 is syntenic to chromosome 21 of *Reinhardtius hippoglossoides* (Greenland halibut), where *sox9a* was suggested as a possible SD candidate gene of this XX/XY species, although other genes, such as *gdf6* and *sox2* in chromosome 10, were also suggested as potential candidates (Ferchaud et al., 2022). The latter gene, *sox2*, would point to a similar SD system to that reported in *Sc. maximus* (Martínez et al., 2021). The syntenic relationships between flatfish adds evidence to the huge heterogeneity of SD systems in Pleuronectiformes, even between closely related species (Drinan et al., 2018; Einfeldt et al., 2021; Ferchaud et al., 2022; Martínez et al., 2021), but also highlights the independent recruitment of major SD drivers from common gene families (e.g., *fshr*, *dmrt*, *amh*, *gsdf* or *sox*) across different fish and vertebrate species (Guiguen et al., 2019; Martínez et al., 2014).

5 | CONCLUSIONS

The chromosome-level *Solea senegalensis* genome assembly reported in this study is among the most contiguous fish assemblies to date. Its integration with previous resources has generated a robust genomic framework for future studies in this important commercial species. This new high-quality assembly enabled the identification of a very consistent SD gene for the species, the follicle stimulating hormone receptor (*fshr*), a new SD gene reported for the first time in Pleuronectiformes. Our hypothesis, supported by functional data, is that the Y-linked variant (*fshry*), through some unknown mechanism, reduces FSH signalling, impeding the down-regulation of *amh* and thus driving the undifferentiated gonad toward testis, although we cannot exclude a putative neofunctionalization of this allelic variant. This information allowed us to validate a molecular tool for sexing, very useful for production and for management of wild populations of *S. senegalensis*.

AUTHOR CONTRIBUTIONS

RH: identification and characterization of the SD gene, and molecular tool for sexing. MH: responsible of genetic map construction and genome scaffolding. JR: responsible for orthology and phylogenetic analyses on candidate genes in flatfish. JGG: genome annotation and collaboration in genome assembly. FC: genome assembly. FR: qPCR analyses on gonad differentiation. RNP: repetitive DNA analysis. AB: bioinformatics support across multiple tasks. PRV: sampling, anatomy and histology of gonads. DT: sampling, anatomy and histology of gonads. PSQ: supervision of anatomy and histology work. DRA: integration of cytogenetic, genetic and physical maps. MER: integration of cytogenetic, genetic and physical maps. AA-P: integration of cytogenetic, genetic and physical maps. IC: anchoring BACs to scaffolds. ND: production of full-sib families for genetic map construction. TMP: collaboration in sampling at Stolt Sea Farm SA. AR: supervision of sampling at Stolt Sea Farm SA. MCDR: 3D protein modelling. DP: 3D protein modelling. AM: planning and design of the study. MG: coordination and supervision of genome sequencing. CB: sex determination comparative genomics in flatfish. DR: gene expression analyses (qPCR and RNA-Seq). LR: coordination of cytogenetic mapping integration. TA: coordination and supervision of genome assembly and annotation. CRR: planning and design of the study. PM: coordination, planning and design of the study; gene expression analysis. Manuscript writing: PM, MH, DR, CB, TA, JGG, FC, PRV. All authors revised the manuscript and contributed to the final version.

ACKNOWLEDGEMENTS

This study was supported by the Spanish Ministry of Economy and Competitiveness, FEDER Grants (RTI2018-096847-B-C21, RTI2018-096847-B-C22 and RTI2018-097110-B-C21), Junta de Andalucía-FEDER Grant (P20-00938) and the European Union's Horizon 2020 research and innovation programme under grant agreement No. 81792 (AQUA-FAANG). We thank Geneaqua SL for their participation and financial support of sequencing. We acknowledge the bioinformatic support of the Centro de Supercomputación de Galicia (CESGA).

CONFLICT OF INTEREST

The authors declare that they have no conflict of interest.

DATA AVAILABILITY STATEMENT

All sequences generated for genome annotation, genetic map construction and gonadal differentiation have been uploaded to ENA (PRJEB47818) and NCBI (PRJNA820527) Bioprojects detailed by sample in the Supporting Table Metadata, which additionally includes biological and analysis information for all samples in this study. Genotypes of offspring and parentals of the three families are provided as a supporting Table named "Genotypes Mapping families."

BENEFIT-SHARING

Benefits from this research accrue from the sharing of our data and results on public databases as described above.

ORCID

Alberto Arias-Pérez https://orcid.org/0000-0001-8967-4519
Paulino Martínez https://orcid.org/0000-0001-8438-9305

REFERENCES

Altschul, S. F., Gish, W., Miller, W., Myers, E. W., & Lipman, D. J. (1990). Basic local alignment search tool. *Journal of Molecular Biology*, *215*, 403–410. https://doi.org/10.1016/S0022-2836(05)80360-2

Baek, M., DiMaio, F., Anishchenko, I., Dauparas, J., Ovchinnikov, S., Lee, G. R., Wang, J., Cong, Q., Kinch, L. N., Schaeffer, R. D., Millán, C., Park, H., Adams, C., Glassman, C. R., DeGiovanni, A., Pereira, J. H., Rodrigues, A. V., van Dijk, A. A., Ebrecht, A. C., … Baker, D. (2021). Accurate prediction of protein structures and interactions using a three-track neural network. *Science*, *373*, 871–876. https://doi.org/10.1126/science.abj8754

Bao, L., Tian, C., Liu, S., Zhang, Y., Elaswad, A., Yuan, Z., Khalil, K., Sun, F., Yang, Y., Zhou, T., Li, N., Tan, S., Zeng, Q., Liu, Y., Li, Y., Li, Y., Gao, D., Dunham, R., Davis, K., … Liu, Z. (2019). The Y chromosome sequence of the channel catfish suggests novel sex determination mechanisms in teleost fish. *BMC Biology*, *17*, 6. https://doi.org/10.1186/s12915-019-0627-7

Buchfink, B., Reuter, K., & Drost, H. G. (2021). Sensitive protein alignments at tree-of-life scale using DIAMOND. *Nature Methods*, *18*, 366–368. https://doi.org/10.1038/s41592-021-01101-x

Cabral, H. N. (2000). Comparative feeding ecology of sympatric *Solea solea* and *Solea senegalensis*, within nursery areas of the Tagus estuary, Portugal. *Journal of Fish Biology*, *57*, 1550–1562. https://doi.org/10.1111/j.1095-8649.2000.tb02231.x

Catchen, J., Hohenlohe, P. A., Bassham, S., Amores, A., & Cresko, W. A. (2013). Stacks: An analysis tool set for population genomics. *Molecular Ecology*, *22*, 3124–3140.

Catchen, J., Hohenlohe, P. A., Bassham, S., Amores, A., & Cresko, W. A. (2020). Chromonomer: A tool set for repairing and enhancing assembled genomes through integration of genetic maps and conserved synteny. *G3- Genes Genomes Genetics*, *10*, 4115–4128.

Chen, S., Zhang, G., Shao, C., Huang, Q., Liu, G., Zhang, P., Song, W., An, N., Chalopin, D., Volff, J. N., Hong, Y., Li, Q., Sha, Z., Zhou, H., Xie, M., Yu, Q., Liu, Y., Xiang, H., Wang, N., … Wang, J. (2014). Whole-genome sequence of a flatfish provides insights into ZW sex chromosome evolution and adaptation to a benthic lifestyle. *Nature Genetics*, *46*, 253–260. https://doi.org/10.1038/ng.2890

Chen, S., Zhou, Y., Chen, Y., & Gu, J. (2018). fastp: An ultra-fast all-in-one FASTQ preprocessor. *Bioinformatics*, *34*, i884–i890. https://doi.org/10.1093/bioinformatics/bty560

Cioffi, M. B., Yano, C. F., Sember, A., & Bertollo, L. A. C. (2017). Chromosomal evolution in lower vertebrates: Sex chromosomes in Neotropical fishes. *Genes*, *8*, 258. https://doi.org/10.3390/genes8100258

Conesa, A., Gotz, S., Garcia-Gomez, J. M., Terol, J., Talon, M., & Robles, M. (2005). Blast2GO: A universal tool for annotation, visualization and analysis in functional genomics research. *Bioinformatics*, *21*, 3674–3676. https://doi.org/10.1093/bioinformatics/bti610

Cui, X., Lu, Z., Wang, S., Wang, J. J.-Y., & Gao, X. (2016). CMsearch: Simultaneous exploration of protein sequence space and structure space improves not only protein homology detection but also protein structure prediction. *Bioinformatics*, *32*, i332–i340. https://doi.org/10.1093/bioinformatics/btw271

Curzon, A. Y., Dor, L., Shirak, A., Meiri-Ashkenazi, I., Rosenfeld, H., Ron, M., & Seroussi, E. (2021). A novel c.1759T>G variant in follicle-stimulating hormone-receptor gene is concordant with male determination in the flathead grey mullet (*Mugil cephalus*). *G3-Genes Genomes Genetics*, *11*, jkaa044. https://doi.org/10.1093/g3journal/jkaa044

de la Herrán, R., Hermida, M., Rubiolo, J., Gómez-Garrido, J., Cruz, F., Robles, F., Navajas-Pérez, R., Blanco, A., Villamayor, P. R., Torres, D., Sanchez-Quinteiro, P., & Ramirez, D. (2022). A chromosome-level genome assembly enables the identification of the follicle stimulating hormone receptor as the master sex determining gene in *Solea senegalensis*. *bioRvix*. https://doi.org/10.1101/2022.03.02.482245

Díaz-Ferguson, E., Cross, I., Barrios, M., Pino, A., Castro, J., Bouza, C., Martínez, P., & Rebordinos, L. (2012). Genetic characterization, based on microsatellite loci, of *Solea senegalensis* (Soleidae, Pleuronectiformes) in Atlantic coast populations of the SW Iberian Peninsul. *Ciencias Marinas*, *38*, 129–142.

Dobin, A., Davis, C. A., Schlesinger, F., Drenkow, J., Zaleski, C., Jha, S., Batut, P., Chaisson, M., & Gingeras, T. R. (2013). STAR: ultrafast universal RNA-Seq aligner. *Bioinformatics*, *29*, 15–21. https://doi.org/10.1093/bioinformatics/bts635

Drinan, D. P., Loher, T., & Hauser, L. (2018). Identification of genomic regions associated with sex in Pacific halibut. *Journal of Heredity*, *109*, 326–332. https://doi.org/10.1093/jhered/esx102

Edvardsen, R. B., Wallerman, O., Furmanek, T., Kleppe, L., Jern, P., Wallberg, A., Kjærner-Semb, E., Mæhle, S., Olausson, S. K., Sundström, E., Harboe, T., Mangor-Jensen, R., Møgster, M., Perrichon, P., Norberg, B., & Rubin, C. J. (2022). Heterochiasmy and the establishment of gsdf as a novel sex determining gene in Atlantic halibut. *PLoS Genetics*, *8*(18), e1010011. https://doi.org/10.1371/journal.pgen.1010011

Einfeldt, A. L., Kess, T., Messmer, A., Duffy, S., Wringe, B. F., Fisher, J., den Heyer, C., Bradbury, I. R., Ruzzante, D. E., & Bentzen, P. (2021). Chromosome level reference of Atlantic halibut *Hippoglossus hippoglossus* provides insight into the evolution of sexual determination systems. *Molecular Ecology Resources*, *21*, 1686–1696. https://doi.org/10.1111/1755-0998.13369

Erdös, G., Pajkos, M., & Dosztányi, Z. (2021). IUPred3: Prediction of protein disorder enhanced with unambiguous experimental annotation and visualization of evolutionary conservation. *Nucleic Acids Research*, *49*, W297–W303. https://doi.org/10.1093/nar/gkab408

Ferchaud, A. L., Mérot, C., Normandeau, E., Ragoussis, J., Babin, C., Djambazian, H., Bérubé, P., Audet, C., Treble, M., Walkusz, W., & Bernatchez, L. (2022). Chromosome-level assembly reveals a putative Y-autosomal fusion in the sex determination system of the Greenland halibut (*Reinhardtius hippoglossoides*). *G3- Genes Genomes Genetics*, *12*, jkab376. https://doi.org/10.1093/g3journal/jkab376

Feron, R., Zahm, M., Cabaum, C., Klopp, C., Roques, C., Bouchez, O., Eché, C., Valière, S., Donnadieu, C., Haffray, P., & Bestin, A. (2020). Characterization of a Y-specific duplication/insertion of the anti-Mullerian hormone type II receptor gene based on a chromosome-scale genome assembly of yellow perch, *Perca flavescens*. *Molecular Ecology Resources*, *20*, 531–543. https://doi.org/10.1111/1755-0998.13133

Ferraresso, S., Bargelloni, L., Babbucci, M., Cannas, R., Follesa, M. C., Carugati, L., Melis, R., Cau, A., Koutrakis, M., Sapounidis, A., Crosetti, D., & Patarnello, T. (2021). *Fshr*: A fish sex-determining locus shows variable incomplete penetrance across flathead grey mullet populations. *iScience*, *24*, 101886. https://doi.org/10.1016/j.isci.2020.101886

Figueras, A., Robledo, D., Corvelo, A., Hermida, M., Pereiro, P., Rubiolo, J. A., Gómez-Garrido, J., Carreté, L., Bello, X., Gut, M., Gut, I. G., Marcet-Houben, M., Forn-Cuní, G., Galán, B., García, J. L., Abal-Fabeiro, J. L., Pardo, B. G., Taboada, X., Fernández, C., … Martínez, P. (2016). Whole genome sequencing of turbot (*Scophthalmus maximus*; Pleuronectiformes): A fish adapted to demersal life. *DNA Research*, *23*, 181–192. https://doi.org/10.1093/dnares/dsw007

Gao, B., Shen, D., Xue, S., Chen, C., Cui, H., & Song, C. (2016). The contribution of transposable elements to size variations between four teleost genomes. *Mobile DNA*, *7*, 4. https://doi.org/10.1186/s13100-016-0059-7

García-Cegarra, A., Merlo, M. A., Ponce, M., Portela-Bens, S., Cross, I., Manchado, M., & Rebordinos, L. (2013). A preliminary genetic map in *Solea senegalensis* (pleuronectiformes, soleidae) using BAC-FISH and next-generation sequencing. *Cytogenetic and Genome Research*, *14*, 227–240. https://doi.org/10.1159/000355001

Guerrero-Cózar, I., Gomez-Garrido, J., Berbel, C., Martinez-Blanch, J. F., Alioto, T., Claros, M. G., Gagnaire, P. A., & Manchado, M. (2021).

Chromosome anchoring in Senegalese sole (*Solea senegalensis*) reveals sex-associated markers and genome rearrangements in flatfish. *Scientific Reports*, *11*, 13460. https://doi.org/10.1038/s41598-021-92601-5

Guiguen, Y., Fostier, A., & Herpin, A. (2019). Sex determination and differentiation in fish: Genetic, genomic, and endocrine aspects. In H.-P. Wang, F. Piferrer, S.-L. Chen, & Z.-G. Shen (Eds.), *Sex control in aquaculture* (Vol. *1*, pp. 35–63). John Wiley & Sons Ltd.

Guindon, S., Dufayard, J. F., Lefort, V., Anisimova, M., Hordijk, W., & Gascuel, O. (2010). New algorithms and methods to estimate maximum-likelihood phylogenies: Assessing the performance of PhyML 3.0. *Systematic Biology*, *59*, 307–321. https://doi.org/10.1093/sysbio/syq010

Haas, B. J., Salzberg, S. L., Zhu, W., Pertea, M., Allen, J. E., Orvis, J., White, O., Buell, C. R., & Wortman, J. R. (2008). Automated eukaryotic gene structure annotation using EVidenceModeler and the program to assemble spliced alignments. *Genome Biololgy*, *9*, R7. https://doi.org/10.1186/gb-2008-9-1-r7

Hao, Z., Lv, D., Ge, Y., Shi, J., Weijers, D., Yu, G., & Chen, J. (2020). *RIdeogram*: Drawing SVG graphics to visualize and map genome-wide data on the idiograms. *PeerJ Computer Science*, *6*, e251. https://doi.org/10.7717/peerj-cs.251

Hattori, R. S., Murai, Y., Oura, M., Masuda, S., Majhi, S. K., Sakamoto, T., Fernandino, J. I., Somoza, G. M., Yokota, M., & Strüssmann, C. A. (2012). A Y-linked anti-Müllerian hormone duplication takes over a critical role in sex determination. *Proceedings of the National Academy of Sciences USA*, *109*, 2955–2959. https://doi.org/10.1073/pnas.1018392109

Hayashi, Y., Kobira, H., Yamaguchi, T., Shiraishi, E., Yazawa, T., Hirai, T., Kamei, Y., & Kitano, T. (2010). High temperature causes masculinization of genetically female medaka by elevation of cortisol. *Molecular Reproduction and Development*, *77*, 679–686. https://doi.org/10.1002/mrd.21203

Herpin, A., Schartl, M., Depincé, A., Guiguen, Y., Bobe, J., Hua-Van, A., Hayman, E. S., Octavera, A., Yoshizaki, G., Nichols, K. M., Goetz, G. W., & Luckenbach, J. A. (2021). Allelic diversification after transposable element exaptation promoted *gsdf* as the master sex determining gene of sablefish. *Genome Research*, *31*, 1366–1381. https://doi.org/10.1101/gr.274266.120

Hu, J., Fan, J., Sun, Z., & Liu, S. (2020). NextPolish: A fast and efficient genome polishing tool for long-read assembly. *Bioinformatics*, *36*, 2253–2255. https://doi.org/10.1093/bioinformatics/btz891

Huerta-Cepas, J., Serra, F., & Bork, P. (2016). ETE 3: Reconstruction, analysis, and visualization of Phylogenomic data. *Molecular Biology and Evolution*, *33*, 1635–1638. https://doi.org/10.1093/molbev/msw046

Ishida, T., & Kinoshita, K. (2007). PrDOS: Prediction of disordered protein regions from amino acid sequence. *Nucleic Acids Research*, *35*, W460–W464. https://doi.org/10.1093/nar/gkm363

Jasonowicz, A. J., Simeon, A. E., Zahm, M., Cabau, C., Klopp, C., Roques, C., Lampietro, C., Lluch, J., Donnadieu, C., Parrinello, H., Drinan, D., Hauser, L., Guiguen, Y., & Planas, J. V. (2022). Generation of a chromosome-level genome assembly for Pacific halibut (*Hippoglossus stenolepis*) and characterization of its sex-determining region. *Molecular Ecology Resources*, *22*, 2685–2700. https://doi.org/10.1111/1755-0998.13641

Jones, D. T., & Cozzetto, D. (2015). DISOPRED3: Precise disordered region predictions with annotated protein-binding activity. *Bioinformatics*, *31*, 857–863. https://doi.org/10.1093/bioinformatics/btu744

Jones, P., Binns, D., Chang, H. Y., Fraser, M., Li, W., McAnulla, C., McWilliam, H., Maslen, J., Mitchell, A., Nuka, G., Pesseat, S., Quinn, A. F., Sangrador-Vegas, A., Scheremetjew, M., Yong, S. Y., López, R., & Hunter, S. (2014). InterProScan 5: Genome-scale protein function classification. *Bioinformatics*, *30*, 1236–1240. https://doi.org/10.1093/bioinformatics/btu031

Kamiya, T., Kai, W., Tasumi, S., Oka, A., Matsunaga, T., Mizuno, N., Fujita, M., Suetake, H., Suzuki, S., Hosoya, S., Tohari, S., Brenner, S., Miyadai, T., Venkatesh, B., Suzuki, Y., & Kikuchi, K. (2012). A trans-species missense SNP in *Amhr2* is associated with sex determination in the tiger pufferfish, *Takifugu rubripes* (Fugu). *PLoS Genetics*, *8*, e1002798. https://doi.org/10.1371/journal.pgen.1002798

Kobayashi, Y., Nozu, R., & Nakamura, M. (2017). Expression and localization of two gonadotropin receptors in gonads of the yellowtail clownfish, *Amphiprion clarkii*. *Journal of Aquaculture & Marine Biology*, *5*, 120. https://doi.org/10.15406/jamb.2017.05.00120

Koyama, T., Nakamoto, M., Morishima, K., Yamashita, R., Yamashita, T., Sasaki, K., Kuruma, Y., Mizuno, N., Suzuki, M., Okada, Y., Ieda, R., Uchino, T., Tasumi, S., Hosoya, S., Uno, S., Koyama, J., Toyoda, A., Kikuchi, K., & Sakamoto, T. (2019). A SNP in a steroidogenic enzyme is associated with phenotypic sex in *Seriola* fishes. *Current Biology*, *29*, 1901–1909.e8. https://doi.org/10.1016/j.cub.2019.04.069

Krzywinski, M., Schein, J., Birol, I., Connors, J., Gascoyne, R., Horsman, D., Jones, S. J., & Marra, M. A. (2009). Circos: An information aesthetic for comparative genomics. *Genome Research*, *19*, 1639–1645. https://doi.org/10.1101/gr.092759.109

Kubista, M., Sindelka, R., Tichopad, A., Bergkvist, A., Lindh, D., & Forootan, A. (2007). The prime technique. Real-time PCR data analysis. *GIT Laboratory Journal*, *9-10*, 33–35.

Langmead, B., Trapnell, C., Pop, M., & Salzberg, S. L. (2009). Ultrafast and memory-efficient alignment of short DNA sequences to the human genome. *Genome Biology*, *10*, R25. https://doi.org/10.1186/gb-2009-10-3-r25

Larkin, M. A., Blackshields, G., Brown, N. P., Chenna, R., McGettigan, P. A., McWilliam, H., Valentin, F., Wallace, I. M., Wilm, A., Lopez, R., Thompson, J. D., Gibson, T. J., & Higgins, D. G. (2007). Clustal W and Clustal X version 2.0. *Bioinformatics*, *23*, 2947–2948. https://doi.org/10.1093/bioinformatics/btm404

Levavi-Sivan, B., Bogerd, J., Mañanós, E. L., Gómez, A., & Lareyre, J. J. (2010). Perspectives on fish gonadotropins and their receptors. *General and Comparative Endocrinology*, *165*, 412–437. https://doi.org/10.1016/j.ygcen.2009.07.019

Li, H. (2011). A statistical framework for SNP calling, mutation discovery, association mapping and population genetical parameter estimation from sequencing data. *Bioinformatics*, *27*, 2987–2993. https://doi.org/10.1093/bioinformatics/btr509

Li, H., & Durbin, R. (2009). Fast and accurate short read alignment with burrows-wheeler transform. *Bioinformatics*, *25*, 1754–1760. https://doi.org/10.1093/bioinformatics/btp324

Li, H., Handsaker, B., Wysoker, A., Fennell, T., Ruan, J., Homer, N., Marth, G., Abecasis, G., Durbin, R., & 1000 Genome Project Data Processing Subgroup. (2009). The sequence alignment/map format and SAMtools. *Bioinformatics*, *25*, 2078–2079. https://doi.org/10.1093/bioinformatics/btp352

Lomsadze, A., Burns, P. D., & Borodovsky, M. (2014). Integration of mapped RNA-Seq reads into automatic training of eukaryotic gene finding algorithm. *Nucleic Acids Research*, *42*, e119. https://doi.org/10.1093/nar/gku557

Lü, Z., Gong, L., Ren, Y., Chen, Y., Wang, Z., Liu, L., Li, H., Chen, X., Li, Z., Luo, H., Jiang, H., Zeng, Y., Wang, Y., Wang, K., Zhang, C., Jiang, H., Wan, W., Qin, Y., Zhang, J., … Li, Y. (2021). Large-scale sequencing of flatfish genomes provides insights into the polyphyletic origin of their specialized body plan. *Nature Genetics*, *53*, 742–751. https://doi.org/10.1038/s41588-021-00836-9

Luckenbach, J. A., Borski, R. J., Daniels, H. V., & Godwin, J. (2009). Sex determination in flatfishes: Mechanisms and environmental influences. *Seminars in Cell & Developmental Biology*, *20*, 256–263. https://doi.org/10.1016/j.semcdb.2008.12.002

Maroso, F., Hermida, M., Millán, A., Blanco, A., Saura, M., Fernández, A., Dalla Rovere, G., Bargelloni, L., Cabaleiro, S., Villanueva, B., Bouza, C., & Martínez, P. (2018). Highly dense linkage maps from 31 full-sibling families of turbot (*Scophthalmus maximus*) provide insights

into recombination patterns and chromosome rearrangements throughout a newly refined genome assembly. *DNA Research*, *25*, 439–450. https://doi.org/10.1093/dnares/dsy015

Martín, I., Carazo, I., Rasines, I., Rodríguez, C., Fernández, R., Martínez, P., Norambuena, F., Chereguini, O., & Duncan, N. (2019). Reproductive performance of captive Senegalese sole, *Solea senegalensis*, according to the origin (wild or cultured) and gender. *Spanish Journal of Agricultural Research*, *17*, e0608. https://doi.org/10.5424/sjar/2019174-14953

Martínez, P., Robledo, D., Taboada, X., Blanco, A., Moser, M., Maroso, F., Hermida, M., Gómez-Tato, A., Álvarez-Blázquez, B., Cabaleiro, S., Piferrer, F., Bouza, C., Lien, S., & Viñas, A. M. (2021). A genome-wide association study, supported by a new chromosome-level genome assembly, suggests sox2 as a main driver of the undifferentiated ZZ/ZW sex determination of turbot (*Scophthalmus maximus*). *Genomics*, *113*, 1705–1718.

Martínez, P., Viñas, A. M., Sánchez, L., Díaz, N., Ribas, L., & Piferrer, F. (2014). Genetic architecture of sex determination in fish: Applications to sex ratio control in aquaculture. *Frontiers in Genetics*, *5*, 340. https://doi.org/10.3389/fgene.2014.00340

Matsuda, M., Nagahama, Y., Shinomiya, A., Sato, T., Matsuda, C., Kobayashi, T., Morrey, C. E., Shibata, N., Asakawa, S., Shimizu, N., Hori, H., Hamaguchi, S., & Sakaizumi, M. (2002). *DMY* is a Y-specific DM-domain gene required for male development in the medaka fish. *Nature*, *417*, 559–563. https://doi.org/10.1038/nature751

Molina-Luzón, M. J., López, J. R., Robles, F., Navajas-Pérez, R., Ruiz-Rejón, C., De la Herrán, R., & Navas, J. I. (2015). Chromosomal manipulation in Senegalese sole (*Solea senegalensis* Kaup, 1858): Induction of triploidy and gynogenesis. *Journal of Applied Genetics*, *56*, 77–84. https://doi.org/10.1007/s13353-014-0233-x

Morais, S., Aragão, C., Cabrita, E., Conceição, L. E., Constenla, M., Costas, B., … Dinis, M. T. (2016). New developments and biological insights into the farming of *Solea senegalensis* reinforcing its aquaculture potential. *Reviews in Aquaculture*, *8*(3), 227–263. https://doi.org/10.1111/raq.12091

Murozumi, N., Nakashima, R., Hirai, T., Kamei, Y., Ishikawa-Fujiwara, T., Todo, T., & Kitano, T. (2014). Loss of follicle-stimulating hormone receptor function causes masculinization and suppression of ovarian development in genetically female medaka. *Endocrinology*, *155*, 3136–3145. https://doi.org/10.1210/en.2013-2060

Myosho, T., Otake, H., Masuyama, H., Matsuda, M., Kuroki, Y., Fujiyama, A., Naruse, K., Hamaguchi, S., & Sakaizumi, M. (2012). Tracing the emergence of a novel sex-determining gene in medaka, *Oryzias luzonensis*. *Genetics*, *191*, 163–170. https://doi.org/10.1534/genetics.111.137497

Nacif, C. L., Kratochwil, C. F., Kautt, A. F., Nater, A., Machado-Schiaffino, G., Meyer, A., & Henning, F. (2022). Molecular parallelism in the evolution of a master sex-determining role for the anti-Mullerian hormone receptor 2 gene (amhr2) in Midas cichlids. *Molecular Ecology*, 1–13. http://doi.org/10.1111/mec.16466

Nakamoto, M., Uchino, T., Koshimizu, E., Kuchiishi, Y., Sekiguchi, R., Wang, L., Sudo, R., Endo, M., Guiguen, Y., Schartl, M., Postlethwait, J. H., & Sakamoto, T. (2021). A Y-linked anti-Müllerian hormone type-II receptor is the sex-determining gene in ayu, *Plecoglossus altivelis*. *PLoS Genetics*, *17*, e1009705. https://doi.org/10.1371/journal.pgen.1009705

Nawrocki, E. P., Burge, S. W., Bateman, A., Daub, J., Eberhardt, R. Y., Eddy, S. R., Floden, E. W., Gardner, P. P., Jones, T. A., Tate, J., & Finn, R. D. (2015). Rfam 12.0: Updates to the RNA families database. *Nucleic Acids Research*, *43*, D130–D137. https://doi.org/10.1093/nar/gku1063

Nawrocki, E. P., & Eddy, S. R. (2013). Infernal 1.1: 100-fold faster RNA homology searches. *Bioinformatics*, *29*, 2933–2935. https://doi.org/10.1093/bioinformatics/btt509

Pan, Q., Feron, R., Yano, A., Guyomard, R., Jouanno, E., Vigouroux, E., Wen, M., Busne, J. M., Bobe, J., Concordet, J. P., et al. (2019). Identification of the master sex determining gene in northern pike (*Esox lucius*) reveals restricted sex chromosome differentiation. *PLoS Genetics*, *15*, e1008013. https://doi.org/10.1371/journal.pgen.1008013

Parra, G., Blanco, E., & Guigo, R. (2000). GeneID in *drosophila*. *Genome Research*, *10*, 511–515. https://doi.org/10.1101/gr.10.4.511

Pertea, M., Pertea, G. M., Antonescu, C. M., Chang, T. C., Mendell, J. T., & Salzberg, S. L. (2015). StringTie enables improved reconstruction of a transcriptome from RNA-Seq reads. *Nature Biotechnology*, *33*, 290–295. https://doi.org/10.1038/nbt.3122

Ramírez, D., Rodríguez, M. E., Cross, I., Arias-Pérez, A., Merlo, M. A., Anaya, M., Portela-Bens, S., Martínez, P., Robles, F., Ruiz-Rejón, C., & Rebordinos, L. (2022). Integration of maps enables a Cytogenomics analysis of the complete karyotype in *Solea senegalensis*. *International Journal of Molecular Sciences*, *23*, 5353. https://doi.org/10.3390/ijms23105353

Ramos, L., & Antunes, A. (2022). Decoding sex: Elucidating sex determination and how high-quality genome assemblies are untangling the evolutionary dynamics of sex chromosomes. *Genomics*, *114*, 110277. https://doi.org/10.1016/j.ygeno.2022.110277

Ramos-Júdez, S., González-López, W. Á., Ostos, J. H., Mamani, N. C., Alemán, C. M., Beirão, J., & Duncan, N. (2021). Low sperm to egg ratio required for successful in vitro fertilization in a pair-spawning teleost, Senegalese sole (*Solea senegalensis*). *Royal Society Open Science*, *8*, 201718. https://doi.org/10.1098/rsos.201718

Raymond, M., & Rousset, F. (1995). GENEPOP (version 1.2): Population genetics software for exact tests and ecumenicism. *Journal of Heredity*, *86*, 248–249. https://doi.org/10.1093/oxfordjournals.jhered.a111573

Rhie, A., Walenz, B. P., Koren, S., & Phillippy, A. M. (2020). Merqury: Reference-free quality, completeness, and phasing assessment for genome assemblies. *Genome Biology*, *21*, 245. https://doi.org/10.1186/s13059-020-02134-9

Robinson, J. T., Thorvaldsdóttir, H., Wenger, A. M., Zehir, A., & Merisov, J. P. (2017). Variant review with the integrative genomics viewer (IGV). *Cancer Research*, *77*, 31–34. https://doi.org/10.1158/0008-5472.CAN-17-0337

Robledo, D., Fernández, C., Hermida, M., Sciara, A., Álvarez-Dios, J. A., Cabaleiro, S., Caamaño, R., Martínez, P., & Bouza, C. (2016). Integrative transcriptome, genome and quantitative trait loci resources identify single nucleotide polymorphisms in candidate genes for growth traits in turbot. *International Journal of Molecular Sciences*, *17*(2), 243. https://doi.org/10.3390/ijms17020243

Robledo, D., Hermida, M., Rubiolo, J. A., Fernández, C., Blanco, A., Bouza, C., & Martínez, P. (2017). Integrating genomic resources of flatfish (Pleuronectiformes) to boost aquaculture production. *Comparative Biochemistry and Physiology Part D: Genomics and Proteomics*, *21*, 41–55. https://doi.org/10.1016/j.cbd.2016.12.001

Robledo, D., Hernández-Urcera, J., Cal, R. M., Pardo, B. G., Sánchez, L., Martínez, P., & Viñas, A. (2014). Analysis of qPCR reference gene stability determination methods and a practical approach for efficiency calculation on a turbot (*Scophthalmus maximus*) gonad dataset. *BMC Genomics*, *15*, 648. https://doi.org/10.1186/1471-2164-15-648

Robledo, D., Ribas, L., Cal, R., Sánchez, L., Piferrer, F., Martínez, P., & Viñas, A. (2015). Gene expression analysis at the onset of sex differentiation in turbot (*Scophthalmus maximus*). *BMC Genomics*, *16*, 973. https://doi.org/10.1186/s12864-015-2142-8

Romero, P., Obradovic, Z., Li, X., Garner, E. C., Brown, C. J., & Dunker, A. K. (2001). Sequence complexity of disordered protein. *Proteins*, *42*, 38–48. https://doi.org/10.1002/1097-0134(20010101)42:1<38::aid-prot50>3.0.co;2-3

Rozen, S., & Skaletsky, H. (2000). Primer3 on the WWW for general users and for biologist programmers. *Methods in Molecular Biology*, *132*, 365–386. https://doi.org/10.1385/1-59259-192-2:365

Sambroni, E., Lareyre, J. J., & le Gac, F. (2013). Fsh controls gene expression in fish both independently of and through steroid mediation. *PLoS One*, *8*, e76684. https://doi.org/10.1371/journal.pone.0076684

Shao, C., Bao, B., Xie, Z., Chen, X., Li, B., Jia, X., Yao, Q., Ortí, G., Li, W., Li, X., Hamre, K., Xu, J., Wang, L., Chen, F., Tian, Y., Schreiber, A. M., Wang, N., Wei, F., Zhang, J., … Chen, S. (2017). The genome and transcriptome of Japanese flounder provide insights into flatfish asymmetry. *Nature Genetics*, *49*, 119–124. https://doi.org/10.1038/ng.3732

Simão, F. A., Waterhouse, R. M., Ioannidis, P., Kriventseva, E. V., & Zdobnov, E. M. (2015). BUSCO: Assessing genome assembly and annotation completeness with single-copy orthologs. *Bioinformatics*, *31*, 3210–3212. https://doi.org/10.1093/bioinformatics/btv351

Slater, G. S., & Birney, E. (2005). Automated generation of heuristics for biological sequence comparison. *BMC Bioinformatics*, *6*, 31. https://doi.org/10.1186/1471-2105-6-31

Stam, P. (1993). Construction of integrated genetic linkage maps by means of a new computer package: JOINMAP. *The Plant Journal*, *3*, 739–744. https://doi.org/10.1111/j.1365-313X.1993.00739.x

Stanke, M., Schoffmann, O., Morgenstern, B., & Waack, S. (2006). Gene prediction in eukaryotes with a generalized hidden Markov model that uses hints from external sources. *BMC Bioinformatics*, *7*, 62. https://doi.org/10.1186/1471-2105-7-62

Taboada, X., Pansonato-Alves, J. C., Foresti, F., Martínez, P., Viñas, A., Pardo, B. G., & Bouza, C. (2014). Consolidation of the genetic and cytogenetic maps of turbot (*Scophthalmus maximus*) using FISH with BAC clones. *Chromosoma*, *123*, 281–291. https://doi.org/10.1007/s00412-014-0452-2

Takehana, Y., Matsuda, M., Myosho, T., Suster, M. L., Kawakami, K., Shin-I, T., Kohara, Y., Kuroki, Y., Toyoda, A., Fujiyama, A., Hamaguchi, S., Sakaizumi, M., & Naruse, K. (2014). Co-option of *Sox3* as the male-determining factor on the Y chromosome in the fish *Oryzias dancena*. *Nature Communications*, *5*, 4157. https://doi.org/10.1038/ncomms5157

Ulloa-Aguirre, A., Zariñán, T., Jardón-Valadez, E., Gutiérrez-Sagal, R., & Dias, J. A. (2018). Structure-function relationships of the follicle-stimulating hormone receptor. *Frontiers in Endocrinology (Lausanne)*, *9*, 707. https://doi.org/10.3389/fendo.2018.00707

Vega, L., Díaz, E., Cross, I., & Rebordinos, L. (2002). Caracterizaciones citogenética e isoenzimática del lenguado *Solea senegalensis* Kaup, 1858. *Boletín. Instituto Español de Oceanografía*, *18*, 245–250.

Viñas, J., Asensio, E., Cañavate, J. P., & Piferrer, F. (2013). Gonadal sex differentiation in the Senegalese sole (*Solea senegalensis*) and first data on the experimental manipulation of its sex ratios. *Aquaculture*, *384–387*, 74–81. https://doi.org/10.1016/j.aquaculture.2012.12.012

Voorrips, R. E. (2002). Mapchart: Software for the graphical presentation of linkage maps and QTLs. *Journal of Heredity*, *93*, 77–78. https://doi.org/10.1093/jhered/93.1.77

Wang, L., Sun, F., Wan, Z. Y., Yang, Z., Tay, Y. X., Lee, M., Ye, B., Wen, Y., Meng, Z., Fan, B., Alfiko, Y., Shen, Y., Piferrer, F., Meyer, A., Schartl, M., & Yue, G. H. (2022). Transposon-induced epigenetic silencing in the X chromosome as a novel form of *dmrt1* expression regulation during sex determination in the fighting fish. *BMC Biology*, *20*, 5. https://doi.org/10.1186/s12915-021-01205-y

Wang, S., Meyer, E., Mckay, J. K., & Matz, M. V. (2012). 2b-RAD: A simple and flexible method for genome-wide genotyping. *Nature Methods*, *9*, 808–810. https://doi.org/10.1038/nmeth.2023

Wen, M., Pan, Q., Jouanno, E., Montfort, J., Zahm, M., Cabau, C., Klopp, C., Iampietro, C., Roques, C., Bouchez, O., Castinel, A., Donnadieu, C., Parrinello, H., Poncet, C., Belmonte, E., Gautier, V., Avarre, J. C., Dugue, R., Gustiano, R., … Guiguen, Y. (2022). An ancient truncated duplication of the anti-Mullerian hormone receptor type 2 geneis apotential conserved master sex determinant in the Pangasiidae catfish family. *Molecular Ecology Resources*, *22*, 2411–2428. https://doi.org/10.1111/1755-0998.13620

Wu, Y., Close, T. J., & Lonardi, S. (2011). Accurate construction of consensus genetic maps via integer linear programming. *IEEE/ACM Transactions on Computational Biology and Bioinformatics*, *8*, 381–394. https://doi.org/10.1109/TCBB.2010.35

Yano, A., Nicol, B., Jouanno, E., Quillet, E., Fostier, A., Guyomard, R., & Guiguen, Y. (2013). The sexually dimorphic on the Y-chromosome gene (*sdY*) is a conserved male-specific Y-chromosome sequence in many salmonids. *Evolutionary Applications*, *6*, 486–496. https://doi.org/10.1111/eva.12032

Zariñán, T., Perez-Solís, M. A., Maya-Núñez, G., Casas-González, P., Conn, P. M., Dias, J. A., & Ulloa-Aguirre, A. (2010). Dominant negative effects of human follicle-stimulating hormone receptor expression-deficient mutants on wild-type receptor cell surface expression. Rescue of oligomerization-dependent defective receptor expression by using cognate decoys. *Molecular and Cellular Endocrinology*, *321*, 112–122. https://doi.org/10.1016/j.mce.2010.02.027

Zhang, Y. (2008). I-TASSER server for protein 3D structure prediction. *BMC Informatics*, *9*, 40. https://doi.org/10.1186/1471-2105-9-40

Zhang, Z., Lau, S. W., Zhang, L., & Ge, W. (2015). Disruption of zebrafish follicle-stimulating hormone receptor (*fshr*) but not luteinizing hormone receptor (*lhcgr*) gene by TALEN leads to failed follicle activation in females followed by sexual reversal to males. *Endocrinology (United States)*, *156*, 3747–3762. https://doi.org/10.1210/en.2015-1039

Zheng, S., Tao, W., Yang, H., Kocher, T. D., Wang, Z., Peng, Z., Jin, L., Pu, D., Zhang, Y., & Wang, D. (2022). Identification of sex chromosome and sex-determining gene of southern catfish (*Silurus meridionalis*) based on XX, XY and YY genome sequencing. *Proceedings of the Royal Society B*, *289*, 20212645. https://doi.org/10.1098/rspb.2021.2645

SUPPORTING INFORMATION

Additional supporting information can be found online in the Supporting Information section at the end of this article.

How to cite this article: de la Herrán, R., Hermida, M., Rubiolo, J. A., Gómez-Garrido, J., Cruz, F., Robles, F., Navajas-Pérez, R., Blanco, A., Villamayor, P. R., Torres, D., Sánchez-Quinteiro, P., Ramirez, D., Rodríguez, M. E., Arias-Pérez, A., Cross, I., Duncan, N., Martínez-Peña, T., Riaza, A., Millán, A. … Martínez, P. (2023). A chromosome-level genome assembly enables the identification of the follicule stimulating hormone receptor as the master sex-determining gene in the flatfish *Solea senegalensis*. *Molecular Ecology Resources*, *00*, 1–19. https://doi.org/10.1111/1755-0998.13750